Leica
MICROSYSTEMS

STELLARIS
CONFOCAL RE-IMAGINED

LIVE IMAGING ACROSS SCALES AND TIME

A guide to advanced and quantitative applications with the STELLARIS confocal platform

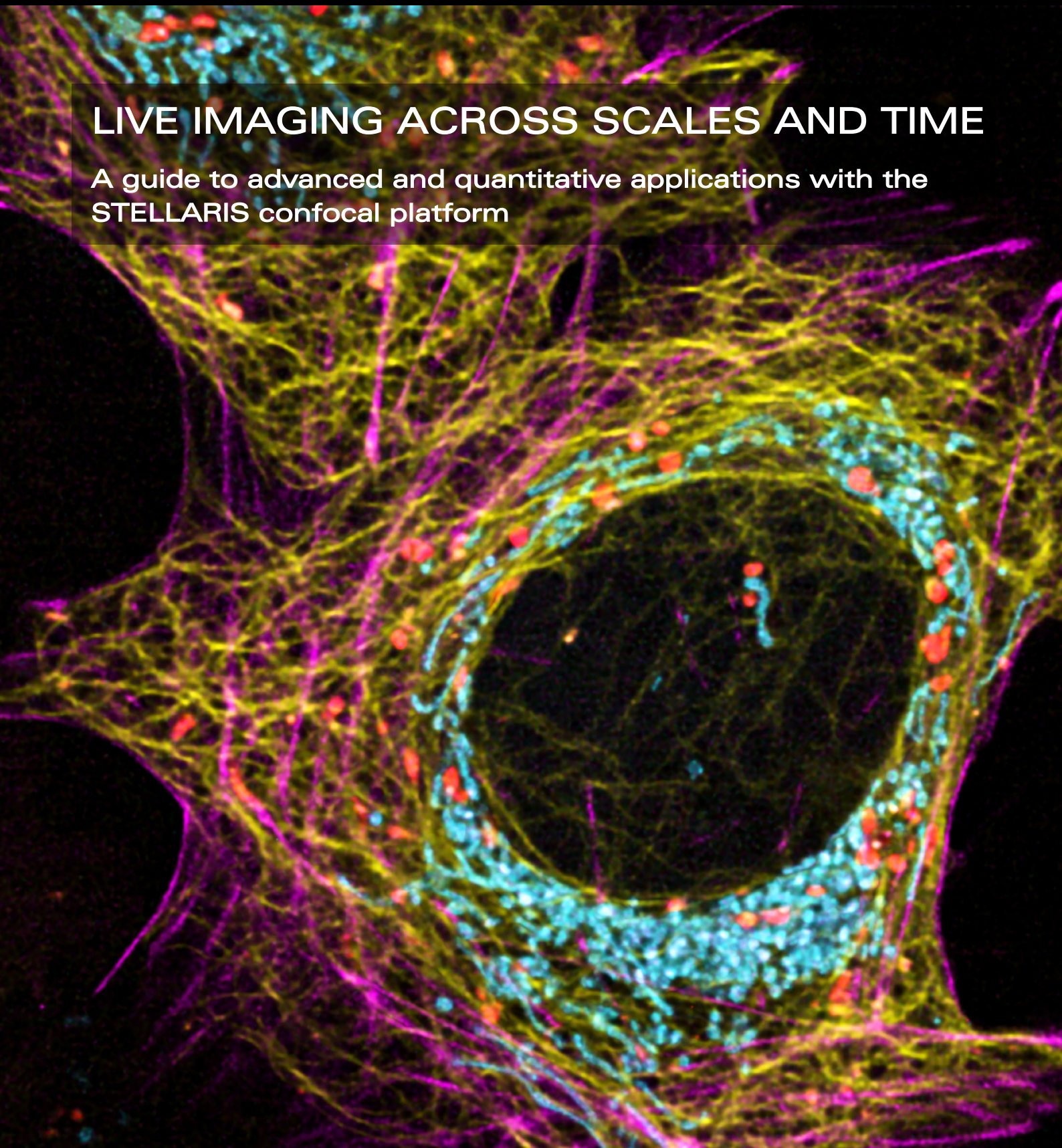

Authors

Judith Reddington, PhD
Dr. Irmtraud Steinmetz
Giulia Ossato, PhD
Dr. Jan Schroeder
Dr. Petra Haas
Dr. Julia Roberti
Dr. Luis Alvarez

Leica Microsystems CMS GmbH

Cover image: High-resolution four-color live cell imaging with STELLARIS. Live mammalian cells labeled with MitoView Green, SPY555-actin, SiR-tubulin, and NIR750 membrane vesicles.

Table of Contents

The value of live cell imaging for research

A fundamental quest in biology is to reveal the interplay of cellular organization, dynamics, and function. Imaging living cells, tissues, and small organisms using fluorescence has proven instrumental in achieving this goal (Fig. 1). Different types of samples and models create different degrees of complexity to explore the dynamic behavior of molecular and cellular networks across scales. Each provides a set of insights that together allow researchers to create a comprehensive view of the mechanisms driving cellular processes, diseases, as well as responses to external inputs (environment, pathogens, drugs, etc.).

There are several challenges that arise from the simultaneous pursuit of imaging depth, speed, and spatial resolution and they are inextricably linked to sample viability. Sample viability is a topic at the forefront of any experiment and critical to ensure a faithful representation of the natural, unperturbed process under study. To generate sound data, it is crucial to match physiological conditions as closely as possible.

For any imaging technology, harnessing the full potential of live cell microscopy requires the expertise to optimize image acquisition conditions so they are minimally invasive. For example, most tissues and cells are never exposed to light in their normal life cycle and it is known that ultraviolet (UV) light damages DNA (Sinha and Häder 2002), focused infrared (IR) light can cause localized heating (Davaji, Richie et al. 2019), and fluorescence excitation can induce (photo)toxicity (Magidson and Khodjakov 2013). In the case of phototoxicity, the responsible are free radical species generated from the reaction between fluorescent proteins or dyes in excited states (generally triplet states) with molecular oxygen or surrounding molecules in cellular components (Tosheva, Yuan et al. 2020). Thus, for live cell imaging, it is best to minimize the production of such species by reducing the amount of excitation light, optimizing the efficiency of the light path, and using detectors that maximize photon collection. Furthermore, an oxygen-depleted environment set at the typical physiological level of a given specimen is highly beneficial to preserve sample health.

The complexity of cells and tissues often requires the use of imaging approaches that provide some degree of optical sectioning to minimize fluorescence contributions from out of focus sources of signal. Confocal microscopy, multiphoton imaging, and light sheet microscopy are such approaches (Fig. 2).

STELLARIS is the next generation of confocal microscopes developed with a focus on live imaging. These microscopes are based on a concept of fully flexible excitation wavelengths and emission detection windows. This enables you to place an excitation line as close as possible to the absorption maximum of any given probe and to have the widest available detection window. This combination maximizes signal generation (photons) as well as photon collection. Moreover, the spectral properties of fluorophores in live cells, tissues, and organisms may differ from those observed when free in solution. The ability to shift excitation or detection windows allows the user to take into account any such changes.

The STELLARIS platform introduced the Power HyD detector family providing a 410 to 850 nm detection window and featuring a proprietary new photon counting approach, namely Power Counting (Schweikhard, Alvarez et al. 2020). Using photon counts for imaging results, instead of the traditional intensities in arbitrary, units ensures advanced quantification. STELLARIS brings this powerful feature as an "everyday imaging" modality without compromising dynamic response or temporal scale. The Power HyD detectors have essentially zero noise and, with a system dead time better than 1.5 ns, they can account for even faint fluorescence.

The following sections show how STELLARIS confocal microscopes can capture and visualize dynamic processes in living samples across scales with exceptional detail. The focus of this article is to provide a guide for choosing the most appropriate imaging technology integrated in the Leica confocal platform for a given type of sample and application and to review how to define the best imaging parameters that keep the specimens healthy throughout the experiment.

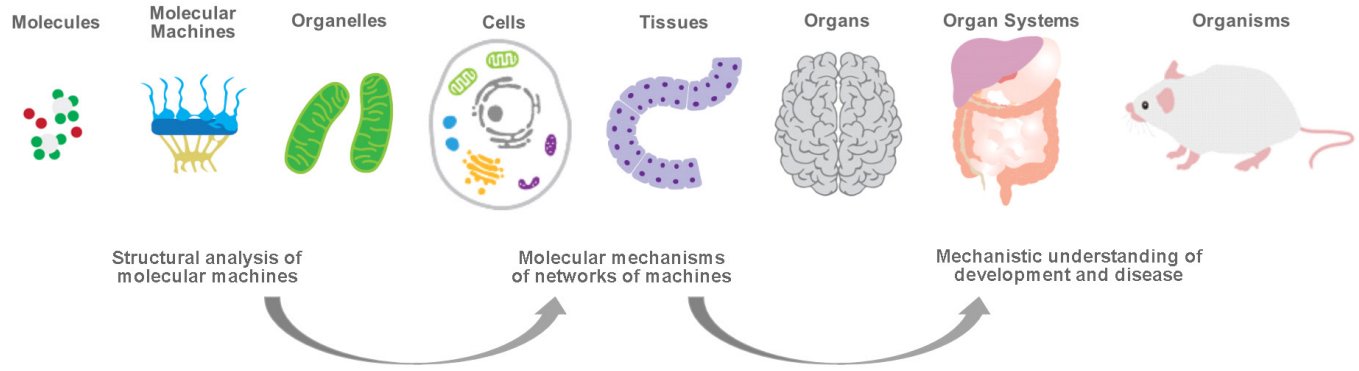

Fig. 1 | From molecules to living organisms: Imaging across scales brings insight into the process under study from different perspectives, enabling "the complete picture" to be obtained.

Fluorescence labeling considerations

There are mainly three ways of adding a fluorescence label in live cell imaging: 1) genetically encoded fluorescent proteins (Bindels, Haarbosch et al. 2017, Rodriguez, Campbell et al. 2017, Matlashov, Shcherbakova et al. 2020), 2) genetic tags used in combination with fluorogenic organic compounds (Gautier, Juillerat et al. 2008, Los, Encell et al. 2008, Tebo, Moeyaert et al. 2021), and 3) organic dyes which are directed to specific intracellular features or organelles (Kilgore, Dolman et al. 2013, Kilgore, Dolman et al. 2014, Lukinavicius, Reymond et al. 2014) or act as probes to follow a particular cellular function (Greenwald, Mehta et al. 2018).

The quality and choice of strategy has the highest impact on the ease of imaging the biological process under study. The brightness and photostability correlate with the amount of excitation needed, but also with the maximal achievable speed. The highest absolute brightness on a sample is modulated by two factors, the number of labels and their intrinsic brightness (molar extinction coefficient ε and quantum yield QY, Valeur 2001). One needs to carefully evaluate the number of fluorophores introduced in a sample. A higher number produces a brighter sample, but also increases the chance of producing phototoxic species from singlet oxygen. Additionally, overexpression of non-endogenous proteins can also lead to perturbations in both cellular process and the microenvironment. Finally, the size and position of the genetic tag should preserve the behavior of the function under study, keeping it close to that of endogenous levels, after the introduction of the tags (Salmon, Carlon-Andres et al. 2020, Willems, de Jong et al. 2020).

When using organic dyes, not only the concentration of the probe, but also the solvent comes into consideration for cellular viability. For example, DMSO -commonly used to solubilize organic dyes- can be very deleterious to biological organisms if not used with care. (Galvao, Davis et al. 2014, Verheijen, Lienhard et al. 2019).

Imaging modalities - Overview

Each imaging system has strengths, choosing the appropriate one strongly depends on the nature of the sample and the biological question. The user should consider the required resolution, acquisition speed, readout sensitivity (signal-to-noise ratio), number of fluorophores or stains, specimen geometry, environmental conditions, and light sensitivity of the sample. To prevent phototoxicity and ensure the most optimal observation conditions, one should set up live cell experiments following the general guidelines 'as much as needed and as little as possible', applied to illumination power (light dose) and sampling rates (time and resolution). The imaging modalities to be considered in this guide are laser scanning confocal, multiphoton, and light sheet microscopy, nanoscopy, and lifetime-based fluorescence imaging.

Confocal microscopy with the STELLARIS 5 and STELLARIS 8 microscopes

The key advantage of confocal microscopy is its optical sectioning capability by means of a pinhole. By limiting the signal coming only from the focal plane (Fig. 2, top panel), the uncertainty of the signal distribution decreases significantly and gives, as a result, sharper images with subcellular resolution (Fig. 2, top) (Sheppard and Wilson 1981, Pawley 2006, Elliott 2020). The optical sections provide information on the three-dimensional distribution of signals by capturing z-stacks (Fig. 2, bottom).

The STELLARIS platform greatly expands the capacity of confocal microscopy for sensitive imaging, thanks to the combination of the white light laser (WLL) excitation, the highly sensitive, photon counting spectral Power HyD detector family (Schweikhard, Alvarez et al. 2020), and a newly optimized beam path. The excitation and detection allow imaging acquisition throughout all the visible spectra extending into the NIR region up to 850 nm. This new extended range can directly enable the use of extra fluorophores in multicolor experiments.

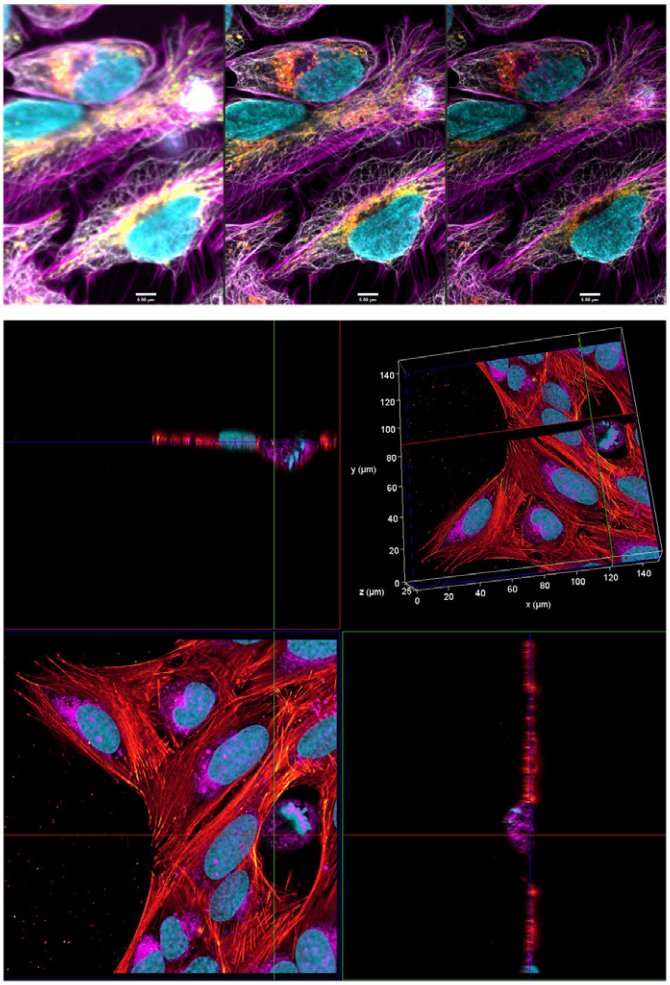

Fig. 2 | Confocal images of mammalian cells. **Top:** 5-color image acquired with STELLARIS at Airy values 4 (open pinhole), 1, and 0.5, respectively. Scale bar: 5 µm. DNA in cyan, tubulin in grey, mitochondria in green, actin in magenta, and Tomm20 in red. **Bottom:** 3D rendering and orthogonal views of a cell stained with Hoechst (nucleus, cyan), Nile Red (internal membranes, magenta), and SiR-actin (actin, glow). SiR-actin is available from Spirochrome.

Excitation, detection, action!

The White Light Laser (WLL)

One of the fundamental elements of the STELLARIS platform is the uniquely flexible excitation as provided by the WLL. The WLL, together with the Acousto-Optical Beam Splitter (AOBS), allows the free selection of the excitation wavelength with nanometer precision from 485 to 685 nm on STELLARIS 5 and from 440 to 790 nm on STELLARIS 8. The WLL can provide up to 8 simultaneous and independent laser lines with a single setting. This flexibility is critical to excite any fluorophore at its excitation optimum and constitutes the first step to minimize the amount of excitation power on a given sample which is paramount in live imaging experiments.

An example of the impact this tunability can have can be seen with mCherry. The classical fixed laser excitation to use with this fluorescent protein would be the 594 nm laser. Nevertheless, at this wavelength you would excite mCherry 14% less than what you can at its absorption maximum at 585 nm. With the WLL you can, hence, get either more excitation with the same laser power or the same photon numbers with less laser power.

Spectral (SP) detection

The detection built into STELLARIS is the ideal complement of the WLL, as it enables the selection of any emission window in front of each of the (up to) five Power HyD detectors (Fig. 3 left). This is possible because the light is spread spectrally through a prism, instead of through a fluorescence filter cube configuration. The prism directs the spatially spread spectra to the detectors and sliders allow a defined portion of the spectra to be selected with nm precision. This ability to choose detection windows of any given spectral width is extremely useful to avoid signal cross talk from nearby fluorophores, but also to define detection windows as wide as possible. This results in a maximal available photon budget. The combination of the WLL and spectral detection geometry in STELLARIS is designed to allow the imaging parameters to be tailored for each experiment and harness as high a photon flux as possible from biological samples. This combination of

excitation at the maximum absorption peak and with the widest possible observation window translates into the ability to lower the needed light dose during acquisition.

The spectral detection approach in STELLARIS is suited for multiplexing by design. It is straight forward to image 5 colors simultaneously using 5 individual WLL lines and five distinct emission windows. Combining these capabilities in multiple sequences makes it straight forward to find optimal excitation and detection windows with a multitude of fluorophore combinations. (Figs. 3, 7, 8, 9, 11, 14, 15, and 17) The filter-less configurations allow the system to adapt to any fluorophore in the visible range. Furthermore, many fluorophores can exhibit sample derived spectral changes. This is particularly true in model organisms or similarly complex samples (ex vivo organ cultures and tissue, organoids, and spheroids). The spectral freedom accounts for any such changes to reach the best possible photon budget with the lowest light dose possible. It is also important to note that another key parameter for live imaging is also favored here for multicolor experiments, speed. Many microscopy systems significantly lose their intrinsic imaging speed when changing from single to multi-color setups, because of the time needed to mechanically change fluorescence filter cubes in and out of the light path. Such loss of speed can be mitigated with the use of triple or quad dichroic mirrors, but such approaches still require at least a line or frame sequential acquisition and prevent any spectral optimization.

The Power HyD detector family

Trying to lower the light dose during live imaging seems obvious as it aims to keep phototoxicity to a minimum. Nevertheless, less excitation usually translates into low photon signals from the samples. Under these conditions, it is easy to be very close to the noise levels of the detectors.

Here the Power HyD detectors with their intrinsic photon counting characteristics excel at imaging sparse dim signals (Bernard M. et al. 2021, Iliopoulou et al. 2018, Freire Rios et al. 2016 and Palczewska et al. 2014). The system dead time of 1.5 ns allows STELLARIS to use photon counting without the need to compromise on imaging speed or dynamic range. In addition, STELLARIS introduced Power Counting where the temporal signature of the detected photons allows the discrimination of two pulses hitting the detector during the dead time (Fig. 4, top panel and Schweikhard, Alvarez et al. 2020 for details). With this technology, it is possible to use photon counting by default while having a signal behavior close to the ideal linear response (Fig. 4, top right). This ability to account for as many photons that reach the detector as possible contributes to the photon efficiency of the STELLARIS platform. One additional benefit here is that the unit of measurement in this case photon counts and not arbitrary units, as is customary in traditional imaging systems. Together with the low noise, it is possible to directly estimate the SNR as the square

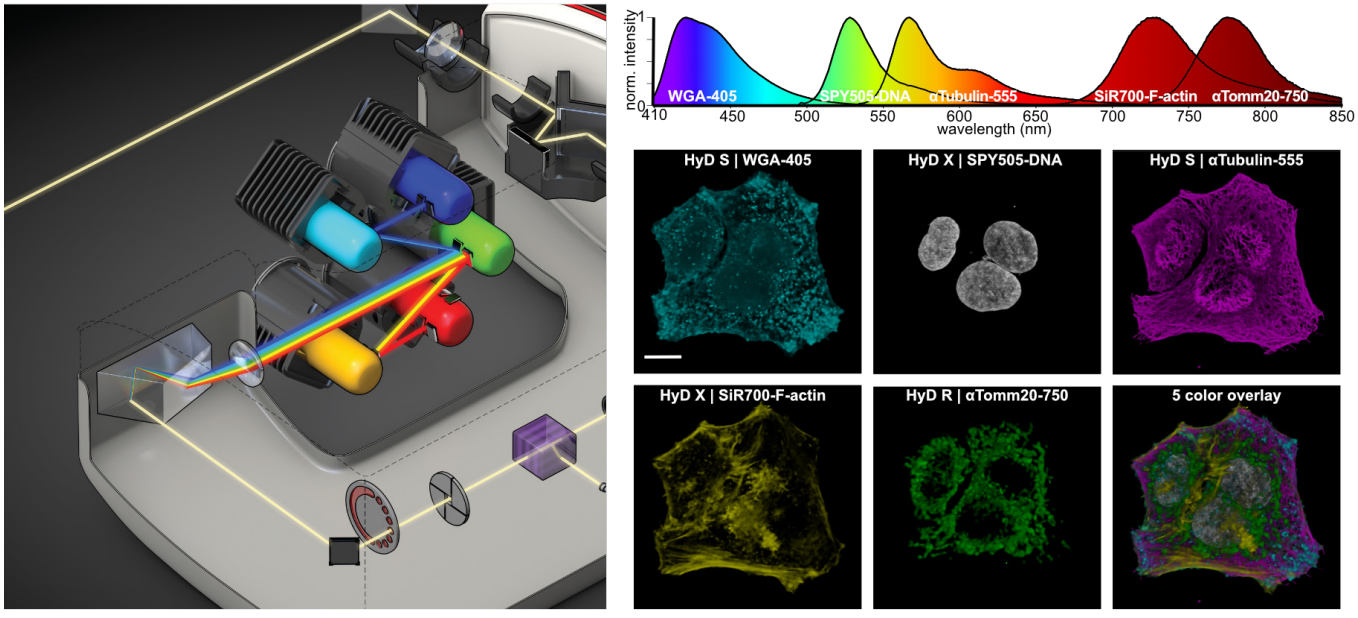

Fig. 3 | STELLARIS spectral detection. **Left:** scan head detail showing the beam path with the prism and spectral detection configuration with 5 Power HyD detectors. **Right:** Mammalian cells stained for five key cellular components. Emission spectra of the fluorophores used and 5-color image of cellular structures with detector types, fluorophores, and targets indicated. Scale bar: 10 µm.

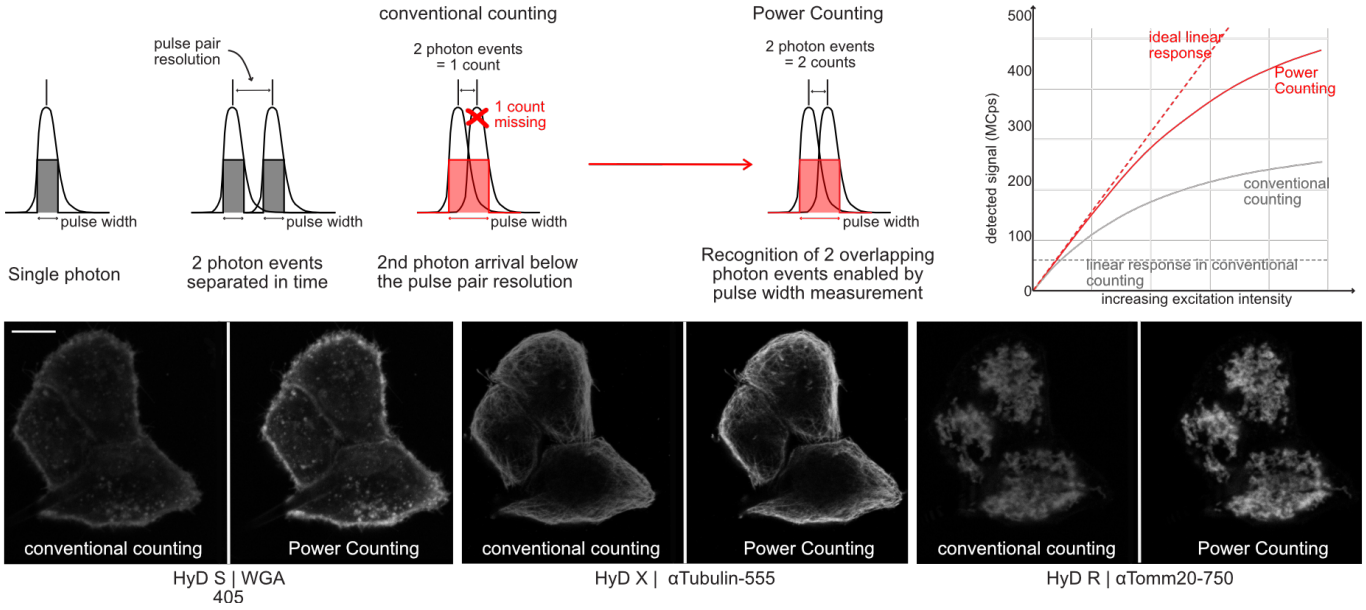

Fig. 4 | **Top:** Power HyD detectors provide added dynamic range and quantifiability through Power Counting technology. Conventional photon counting misses a second photon event occurring within the pulse-pair resolution time; Power Counting correctly accounts for the second photon by using the pulse width information.
Top left: Power Counting signals (red solid curve) as a function of excitation intensity show enhanced dynamic range compared to conventional counting (gray curve).
Bottom: Images of cellular structures recorded without or with Power Counting. Power Counting delivers brighter, crisper images and additional details. Scale bar: 10 µm.

root of the photon counts. Fig. 4 shows the increase in signal that can be harnessed with this new approach. In these examples, the conventional and Power Counting images are shown with the same look up table to make it possible to see the differences in the signal, but also their typical noise. Indeed, another key benefit provided with this detection is a very low noise. It is then possible to use either line or frame accumulation to increase the signals without significantly adding noise. The ability to use an accumulation strategy is a very important tool for live imaging.

If for a given sample, it is not possible to increase the excitation power without inducing cellular damage, signal accumulation can improve the observed fluorescence.

LAS X Navigator: A GPS for sample exploration

Another challenge of live imaging is the need to explore the spatial distribution of signals across scales. It is important to find the relevant parts of the sample to image but spending a long time exploring a live sample trough the oculars with the help of epi-fluorescence can be deleterious to the viability of samples. When imaging tissues, organs, or certain animal models, observing fine structures through the eyepieces is very challenging. It can also be difficult to be certain that a given position is suitable without looking elsewhere first.

LAS X Navigator makes exploring samples and navigating them a breeze. Here the system allows researchers to create a low-resolution overview of the sample in fluorescence and with optical sectioning. This creates a map linked to the physical position of the microscope stage. From here a researcher can move to any position of the sample and create multi-position or tile scan experiments. Each experiment chosen within Navigator can make use of STELLARIS' multi-dimensional acquisition (xyzt and lifetime-based dimensions).

With LAS X Navigator it is then possible to concentrate on the relevant parts of the sample and lower the time spent exploring it. Using Navigator also makes it easier to get a statistically significant number of acquisitions for scientific quantification of events. Finally, thanks to the overview, it is possible to have the sample context for individual acquisitions (Fig. 5).

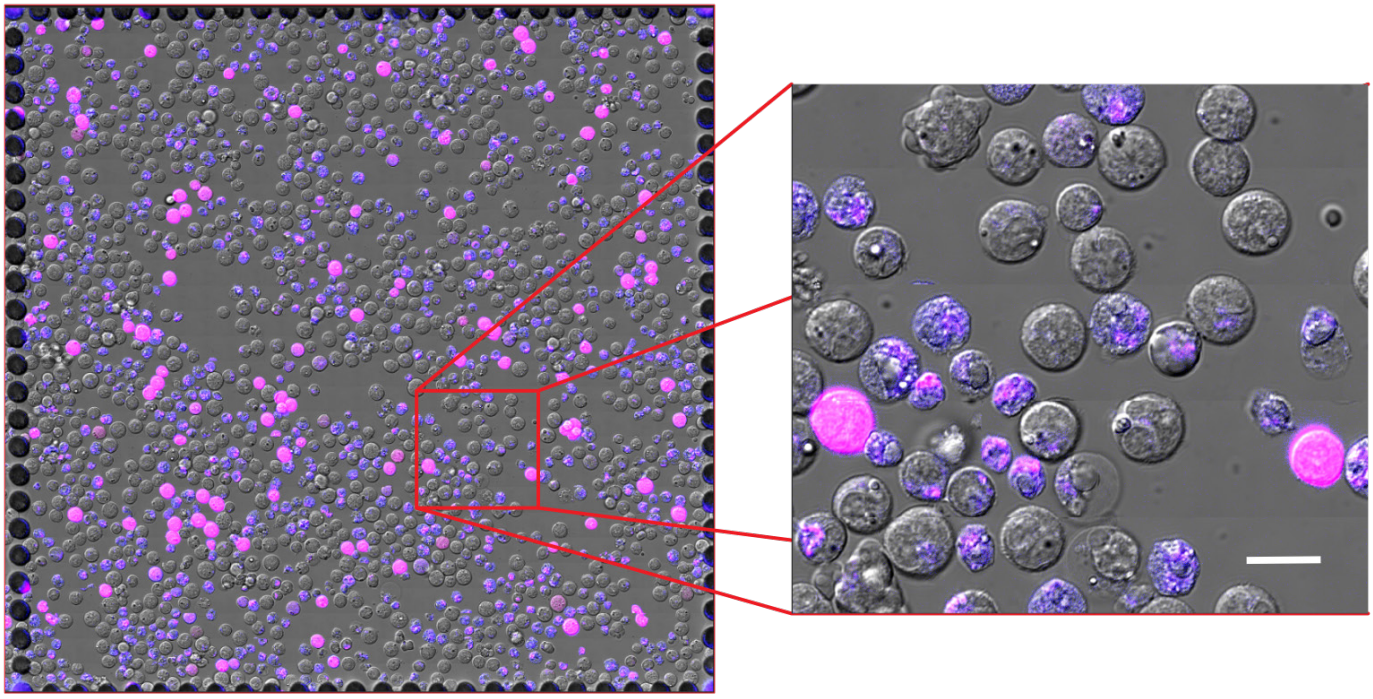

Fig. 5 | Navigator overview from a single 500 µm grid square. DIC image with eCALWY Zn biosensor (blue) and Propidium iodide (PI - magenta) signals. Only the eCALWY positive, PI negative cells with a proper morphology from the DIC image are suitable to assess Zn^{2+} channel function. Scale bar: 5 µm. (For experimental details see Anzilotti et al. Nat. Immuno. 2018).

Life happens in 3D – fast volumetric confocal imaging

Live imaging experiments are a balancing act between sufficient image quality and preserving the health of the specimen, but also the temporal dynamics of the processes of interest. Even if a proper signal can be acquired at a given speed, if the structure of interest moves faster than the acquisition speed, the result will be a deterioration of image quality and resolution. Standard field-of-view scanners are based on galvo mirrors. They have the maximum flexibility combination of scan zoom and speeds. These scanners can use the full field of view (FOV, with field diameter of 22 mm) with speeds up to 600 Hz. This translates into 2.29 frames per second (fps) for a 512x512 image. It is possible to have higher scan speeds, but they require some restriction on the usable FOV. Scanning at 1400 Hz, for example, can provide 512x512 images at 5.21 fps, nevertheless at this speed at least a 4.5 scan zoom is required (see Fig. 6 in the next section and Fig. 15 in the nanoscopy section for examples with the Field-of-view scanner).

In order to maintain a large FOV and increase speed, it is possible to use a resonant scanner that allows significantly higher scan speeds. It is possible to equip STELLARIS systems with either an 8 kHz or 12 kHz scanner (see table for technical details). With these scanners, it is then possible to reach 28 fps and 40 fps with minimal loss of FOV size (see table on the next page for details). This additional speed provides the necessary tool to track faster cellular objects and processes.

In addition, the three-mirror scan configuration in STELLARIS also allows these resonant scanners to use higher frame resolutions ensuring proper sampling at high speeds. This is necessary to avoid a decrease in resolution at these speeds. Although it is possible to image many biological processes on a single plane, volume imaging is often needed to faithfully follow the spatiotemporal changes of sub-cellular components and proteins (Fig. 6 and Fig. 18 in the TauSense section). Here is where the resonant scanner excels as it allows for fast z-stack acquisitions. An increase in acquisition speeds often leads to dimer signals. This lower signal can be compensated by an increase of excitation power, nevertheless this should be a last resort for image optimization during live imaging experiments. It is worth keeping in mind that, at low light levels, the noise floor of the system is a key limiting factor for observing signals. STELLARIS provides a series of dedicated software tools to deliver high quality results from acquisitions done at extremely low excitation light dose and/or high temporal resolution: Dynamic Signal Enhancement (DSE) with its unique AiviaMotion functionality and LIGHTNING (see the following sections for details).

Scanner type	Field-of-view	8 kHz	12 kHz
Bidirectional speed	2 to 5200 Hz (variable)	16 kHz	24 kHz
Scan zoom	0.75-48x	1.24-48x	2-48x
Maximal frame rate 512 x 512	10 fps	28 fps	40 fps
Maximal frame rate 512 x 16	216 fps	282 fps	423 fps
Maximal frame resolution	8192 x 8192	2496 x 2496	1664 x 1664

Scan speeds for the STELLARIS microscopes

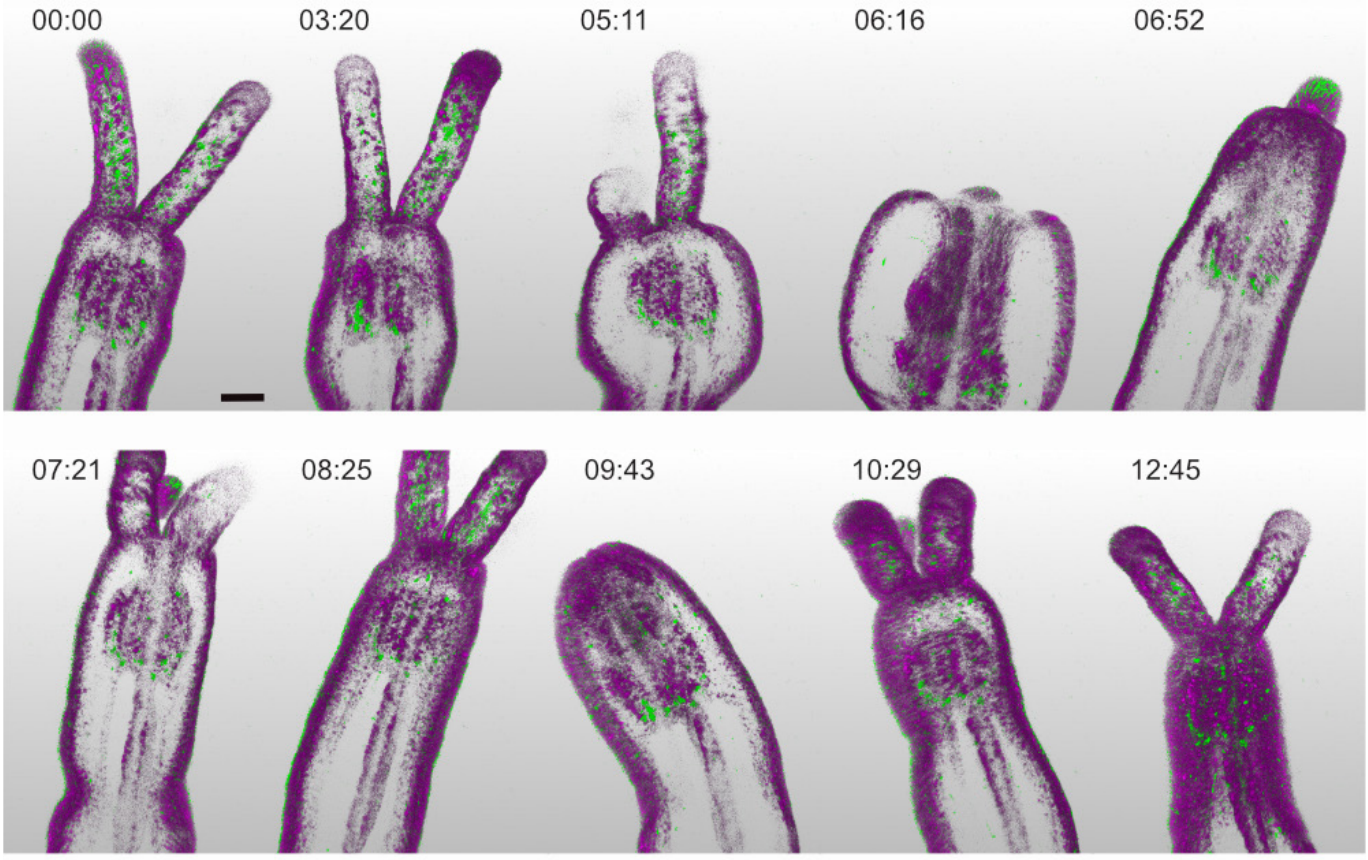

Fig. 6 | Fast resonant scanner 3D-in vivo imaging of *Nematostell a vectensis* (Cnidaria) showing endogenous nematosomes, clusters of freely-circulating cnidocytes (green), and Dextran Red fluorescence (magenta). Endogenous signals and labeled fluorescence separated by TauGating on HyD S (Roberti et al. 2020). A total of 340 volumes were acquired in 12m 45s, one volume every 2.2 seconds. Scale bar: 50 µm. Sample courtesy of Anniek Stokkerman and Aissam Ikmi, EMBL Heidelberg, Germany. Video available at. https://www.leica-microsystems.com/stellaris-fast-3d-nematostella.

Dynamic signal enhancement (DSE) and AiviaMotion

DSE is a powerful tool for the denoising of images. DSE calculates in real-time a moving average (or accumulation when detectors are in photon counting mode) over the raw data to increase the signal-to-noise ratio while preserving temporal resolution. As a result, DSE enables imaging of fast biological events in detail while the structures and objects in the sample move. Although not limited to resonant scanning speeds, the short dwell times in these configurations and their inherited higher noise benefit greatly from DSE (Fig. 7).

Other cases that would benefit from the use of DSE tools is when imaging label-free endogenous signals where photons are very sparse and dynamics are high. DSE can be used, for example, to improve the imaging of intravital blood flow using third harmonic generation (THG) signals on a STELLARIS DIVE multiphoton microscope (see the 70 fps, two-color movie with Tyh1-eYFP for cortical neurons and THG for erythrocytes at https://webcdn.leica-microsystems.com/uploads/tx_leicaproducts/signal-enahncement-dive.mp4).

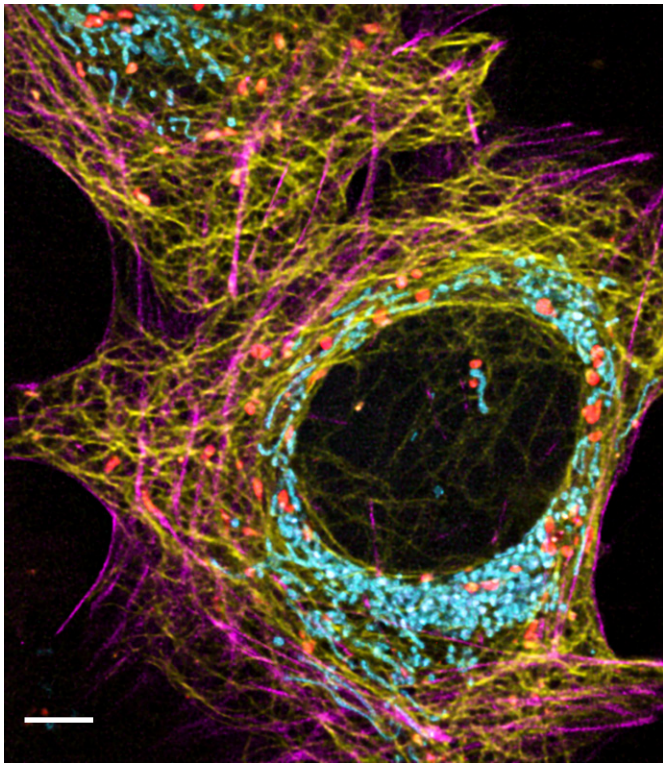

Fig. 7 | Mammalian cells labeled with MitoView Green, SPY555-actin, SiR-tubulin, and NIR750. Simultaneous multi-color imaging with STELLARIS using the FOV scanner. Image series further enhanced by DSE (with AiviaMotion) and LIGHTNING. Scale bar: 10 µm.

The limit to this approach becomes visible when the sample's dynamics are faster than the sampling rate. Differences between raw data frames used for calculation of the rolling window can be large. This, in turn, might lead to so-called ghosting effects when DSE is applied. When this happens, a given signal being averaged out over multiple frames yields artificially elongated signals. It is because of this that it is not possible to just increase the number of frames used in DSE to increase the signal-to-noise ratio.

A natural response of the user would be to lower the number of frames used for calculating the rolling window. However, there will be a trade-off between keeping the dynamics of the sample to avoid ghosting (use of fewer frames) and achieving a good signal-to-noise ratio for the output image (use of more frames). To address this challenge, Leica Microsystems has developed and implemented a new artificial intelligence (AI) feature for the DSE termed AiviaMotion. While the "regular" DSE only uses the acquired, raw data frames as an input for the rolling window, activating AiviaMotion leads to the calculation of additional, interpolated frames as input for the rolling window. More precisely, these additional "AiviaMotion frames" are interlaced between "raw frames" and are calculated by a convolutional neural network (deep learning). With this tool, the "real" frames, but also the "AiviaMotion" ones (AI interpolated frames), are used as input for the DSE. It is then possible to achieve a better signal-to-noise ratio for the same temporal resolution of DSE alone. Alternatively, the experimenter can also lower the number of "real" frames needed for calculating the rolling window and, thus, achieve a certain signal-to-noise ratio with a better temporal resolution. In short, with AiviaMotion it is possible to outsmart the inverse proportion of the temporal resolution and signal-to-noise ratio of a rolling window in your favor.

The LIGHTNING detection concept

To allow users to maximize the resolution and contrast that can be extracted from live cell imaging experiments, Leica Microsystems has developed and integrated LIGHTNING into the STELLARIS platform. LIGHTNING is an adaptive deconvolution process that leverages the Power HyD detectors and imaging characteristics of STELLARIS. LIGHTNING integrates both

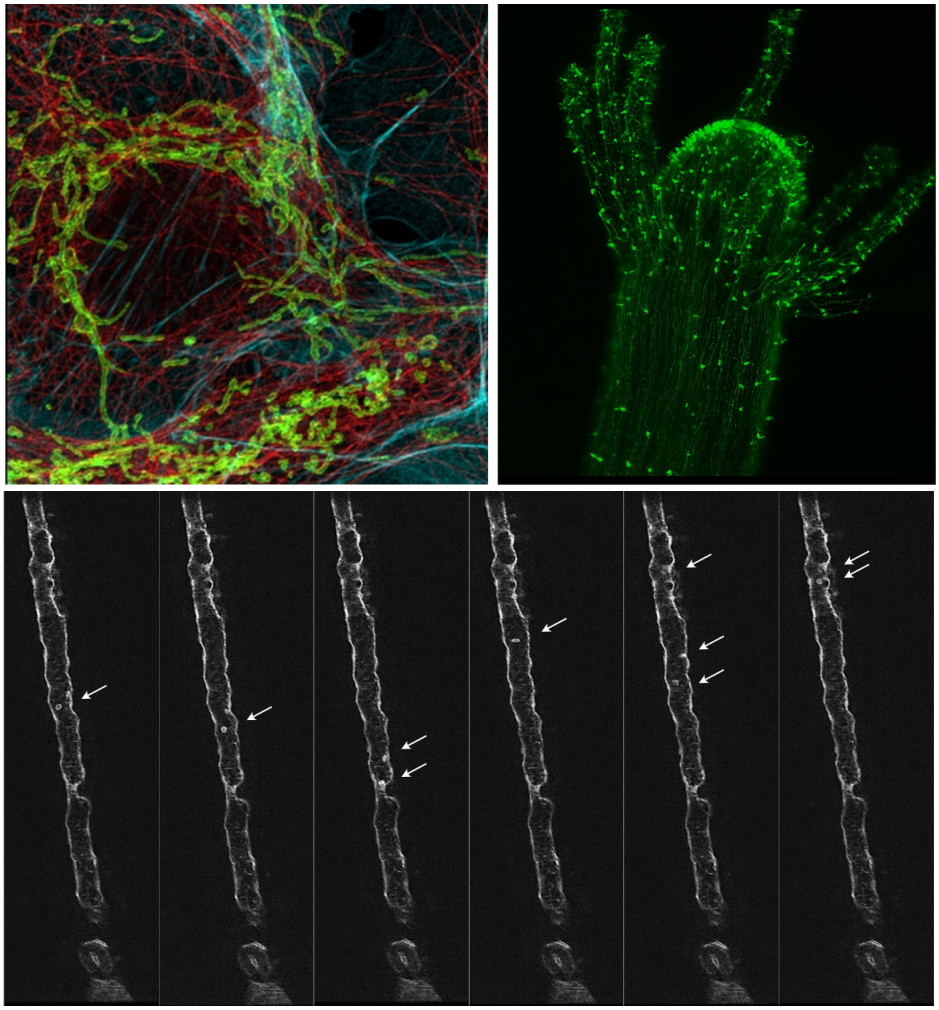

Fig. 8 | **Top left:** live mammalian cells labeled Mitotracker-green, SPY-555 actin and SIR-Tubulin. High resolution imaging on STELLARIS 5 with Power HyD S detectors and LIGHTNING – scale bar 2 µm. **Top right:** Hydractinia expressing eGFP under the control of neurogenesis-related gene labels. Imaging with DLS and LIGHTNING. Sample courtesy of Eleni Chrysostomou, National University of Ireland, Galway, Ireland. **Bottom:** Blood flow in zebrafish embryo. Arrows indicate erythrocytes. Imaging with DLS and LIGHTNING. Sample courtesy of Elvire Guiot and Julien Vermot, IGBMC Imaging Center, France.

the hardware control and software into one easy intuitive wizard. This combination can help reveal fine structures and details of dynamic events, otherwise difficult to single out from the raw data, in a fully automated way. in a fully automated way. For more details, read this white paper.

Unlike traditional deconvolution techniques, that use a global set of parameters for the full image, LIGHTNING calculates an appropriate set of parameters for each voxel to uncover details with the highest fidelity down to 120nm in lateral resolution (Fig. 8). This additional resolution can only be achieved when the appropriate oversampling parameters are used for image acquisition. For cellular imaging and other similar samples, the sampling criteria and signal-to-noise ratio needed to increase the resolution through deconvolution would translate into acquisition speeds and excitation powers seldom compatible with live imaging (see the section on nanoscopy for a more detailed discussion).

Although deconvolution approaches are often used for the sole purpose of increasing resolution, the deconvolution process is meant to reduce contributions from unwanted signals like background and noise. These steps in adaptive deconvolution are independent of the sampling and of particular importance when dealing with dim samples, such as the ones found when following very fast dynamic events with the resonant scanner or in a light sheet microscopy configuration (Fig. 8).

LIGHTNING maintains the full framerate of the STELLARIS systems for up to five channels simultaneously and, therefore, allows subcellular dynamics that occur even on the millisecond timescale to be captured.

LIGHTNING is fully compatible with DSE and the processing of both can be automatically linked when starting acquisition (Fig. 7).

Multiphoton microscopy with DIVE (Deep In Vivo Explorer)

Multiphoton excitation brings key unique advantages for live imaging. This modality is traditionally used for intravital microscopy, large tissue samples (for penetration depth), and label-free imaging. The multiphoton excitation spot geometry provides intrinsic optical sectioning in the absence of a confocal pinhole. This, combined with the use of non-descanned detection paths, allows to minimize the number of optical elements between the fluorescence emission and the detectors. The wavelengths of infrared lasers employed in multiphoton microscopy induce less phototoxicity compared to the corresponding one photon excitation and enable higher penetration depths into scattering samples. In multiphoton microscopy, it is then possible to perform live imaging beyond 1 mm in depth (see Fig. 9) in tissues, model organisms, animals, and plants (Sun, Haberman et al. 2017, Lecoq, Orlova et al. 2019, Sheppard 2020).

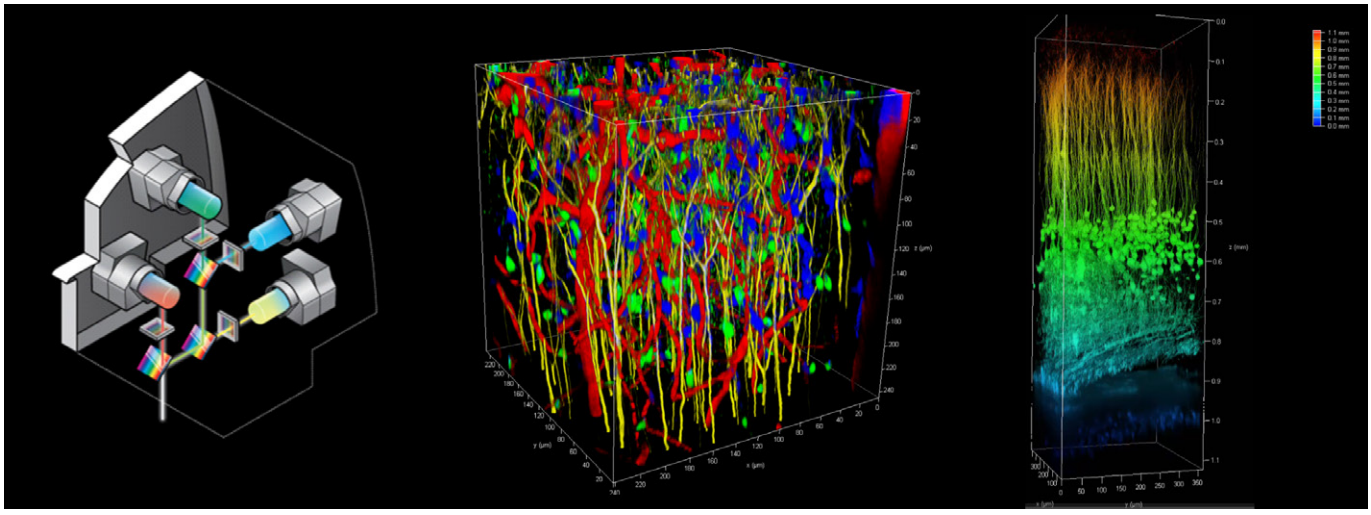

Fig. 9 | **Left:** detection geometry of the 4Tune detector module, showing 4 NDD detectors with the corresponding sliding spectral dichroic mirrors and filters. **Middle:** Live mouse brain showing astrocytes (Sulforhodamine – blue), microglia (GFP – green), neurons, (YFP – yellow), and blood vessels (Alexa680-Dextran – red). **Right:** 1.1-mm-deep image of mouse brain cortex, Thy1-eYFP, color coded for depth. Sample courtesy of LMF, DZNE, Bonn, Germany.

Additionally, multiphoton excitation is particularly advantageous to investigate biological changes from the emission of naturally occurring endogenous fluorophores (NADH, FAD, flavins, porphyrins, retinoids), because the one photon alternative falls in the UV range and is incompatible with sample viability. When paired with fluorescence lifetime imaging microscopy (FLIM), this label-free imaging allows monitoring metabolic changes (Fig. 10 – see details in Wang, Gurlo et al. 2021). Details on lifetime-based imaging applications can be found in the corresponding section on page 20.

The multiphoton excitation affords access to label free structural imaging with the use of second and third harmonic signals (SHG and THG) further extending the label-free imaging capabilities. The use of SHG is particularly suitable to see structural context in tissue as it renders collagen or muscle fibers visible (Fig. 11). THG is especially suitable to follow red blood cells and, thus, is an invaluable tool for vascular related research in animal models. These signals contain essentially null lifetime signatures, so the new lifetime-based tools of STELLARIS are well positioned to improve the access and usefulness of these signals. For more details read the Application note.

STELLARIS DIVE microscopes offer flexible excitation wavelengths with lasers fully tunable in wavelength ranging from 680 up to 1300 nm. In addition to this intrinsic excitation tunability, the STELLARIS 8 DIVE microscope offers fully tunable multicolor emission detection with its 4TUNE non-descanned detection module (Fig. 9). This unique approach to multiphoton detection allows users to freely set the emission detection windows, maximizing photon collection efficiency and enabling even complex multicolor experiments (Fig. 10).

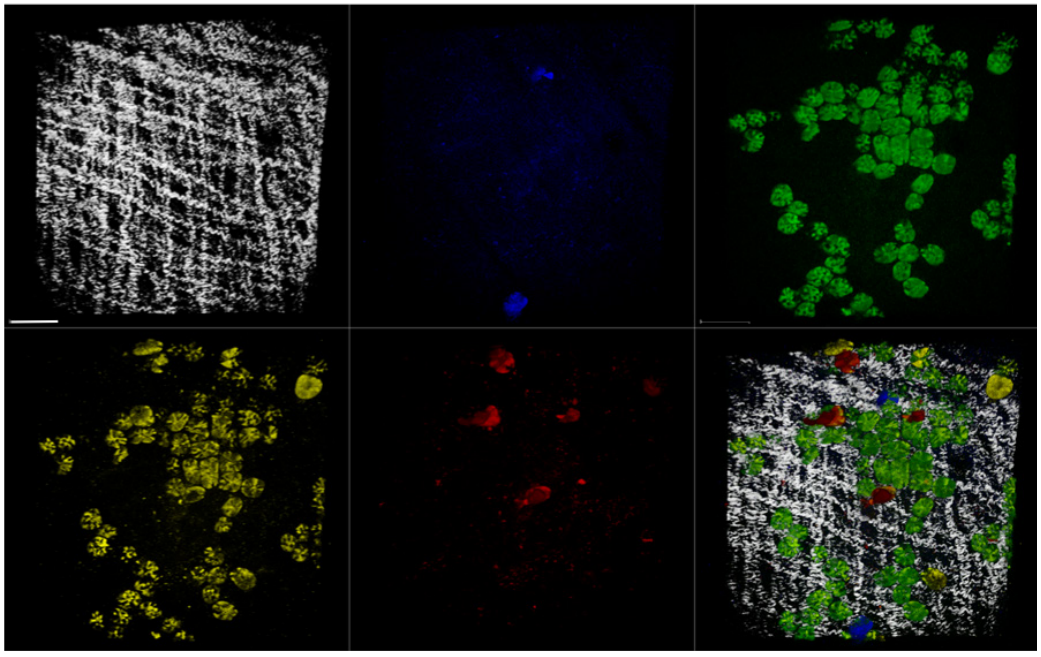

Fig. 10 | Confetti mouse, small intestine showing collagen (SHG – gray), stem cells (green), and cellular progeny of stem cells (red, blue and yellow). Scale bar: 100 µm. Sample courtesy of Jacco van Rheenen, University of Utrecht, the Netherlands.

From a practical point of view, fine tuning of excitation wavelengths and detection windows on the DIVE is key for optimized live imaging. It allows to excite very close to the peak excitation and collect more fluorescence signal from the sample, thus limiting as much as possible the irradiation time and energy needed to produce a given image.

To overcome challenges, such as small movements during live animal observations, an 8-kHz tandem scanner is used for high-speed acquisition. The fast acquisition regimes benefit from specialized STELLARIS imaging modes, such a DSE, LIGHTNING, and AiviaMotion (see the corresponding section for details).

Just like in cells, some endogenous signals, such as FAD/NADH, can be exploited for functional imaging in intravital and tissue imaging (Fig. 11). These specimens do contain a more complex set of endogenous signals and it might at times be desirable to separate such signals from the fluorescent markers/stains used to track the biological processes of interest. The integration of FLIM capabilities in DIVE with FALCON can be leveraged in these cases. It is possible to use phasor separation to single out the signals of interest from other endogenous fluorescence contributions.

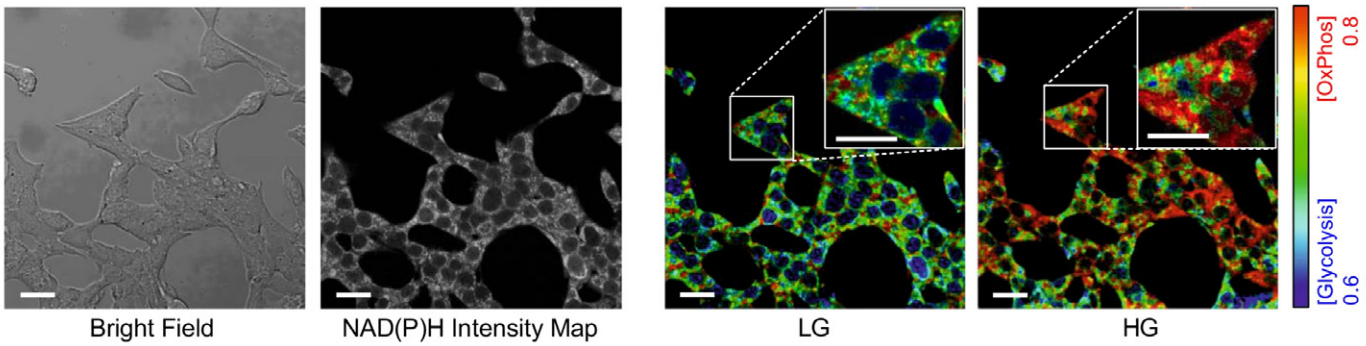

Fig. 11 | Exploring cellular metabolism from the endogenous NAD(P)H signals imaged on a DIVE microscope and analyzed from their fluorescence lifetime behavior. Images showing the low glucose (LG) and high glucose (HG) states for these cells. Color LUT corresponds to glycolysis or oxidative phosphorylation states (adapted from Wang, Z et al 2021).

Light sheet microscopy with DLS (Digital LightSheet)

Light sheet microscopy, where the excitation light is restricted to illuminate the plane being imaged, has enabled imaging fast biological processes in sensitive organisms over extended periods of time (Weber and Huisken 2011, Wan, McDole et al. 2019, Lemon and McDole 2020). This relatively new approach is particularly suited for applications in developmental biology, as it combines exceptionally high imaging speeds, good resolution, and optical sectioning, while minimizing light-induced damage to the specimen. By illuminating only the optical plane being imaged, it is generally considered that 20 times less illumination energy is delivered in a light sheet configuration compared to a regular epi-fluorescence beam (Reynaud, Kržič et al. 2008).

The STELLARIS 5 DLS and STELLARIS 8 DLS microscopes offer light sheet and confocal capabilities in one platform by turning light sheet microscopy vertically. It makes use of the unique TwinFlect mirrors, a Leica invention. Here the confocal scanner and lasers are used to generate a light sheet at a 90° angle with respect to the confocal plane (Köster and Haas 2015). This configuration integrates the illumination and detection beam path into the vertical axis of an inverted confocal microscope without compromising confocal functionality or light sheet quality (Fig. 12).

The DLS is a good live imaging option for samples with geometries requiring gentle volumetric imaging, such as organoids or spheroids and small model organisms like zebrafish, C. elegans, *Drosophila melanogaster*, or Cnidaria (Figs. 8, 12 and 13).

The volumetric speed of DLS allows functional imaging of zebrafish (Fig. 13 left panels - Mattern et al. 2020). Such quantitative approaches would be suitable also for other small model organisms (*C. elegans* and *Drosophila melanogaster*).

In addition to traditional light sheet approaches, the integration of DLS in STELLARIS also offers access to photomanipulation capabilities by default. Photomanipulation makes it possible to perform wound healing assays as well as photoinducible pulse-chase experiments (see Fig. 13 right panels).

One of the challenges of light sheet microscopy is the sample preparation, as the geometry requires very specific mounting strategies. Based on an inverted microscope, the DLS requires little adaptation in this regard as the light sheet is generated from the bottom through an optical glass bottom and brought perpendicularly into the sample when the DLS mirrors on the condenser arm are put in position from either side of the sample (Fig 12).

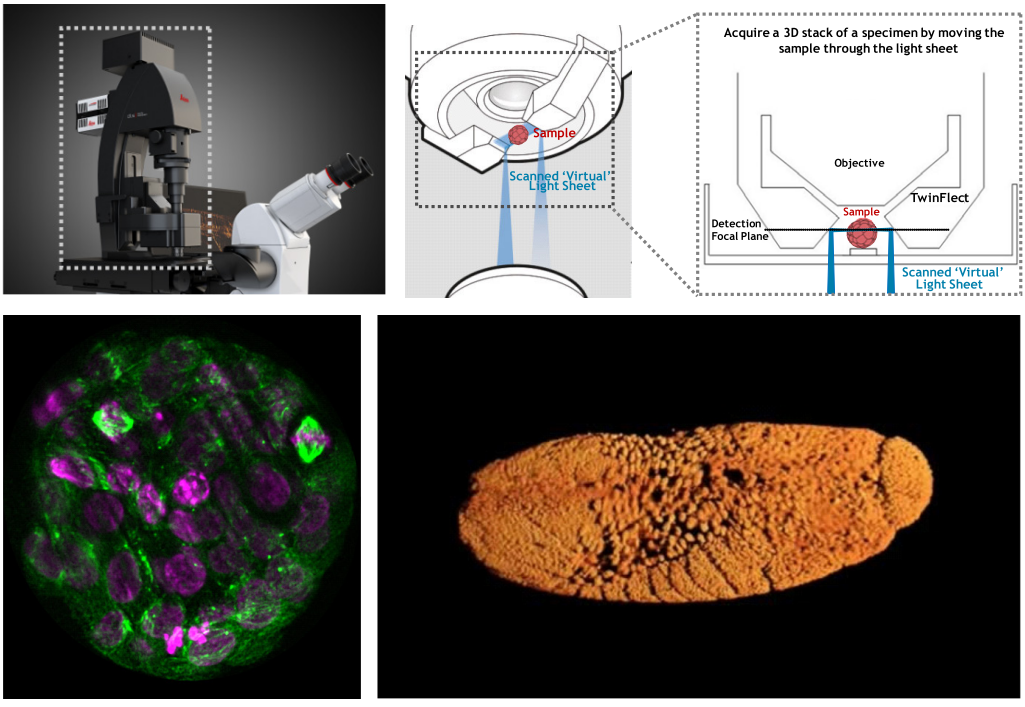

Fig. 12 | **Top:** DLS principle and light path geometry. **Bottom left:** Mammary epithelial micro spheroid cultured in 3D using MCF10A H2B-GFP cell line (Zev Gartner/UCSF) stained with SiR-tubulin. Sample courtesy of B. Eismann and C. Conrad at BioQuant/DKFZ, Heidelberg, Germany. **Bottom right:** Low phototoxicity and specimen imaging in 3D: Development of Drosophila melanogaster over six hours. Probe is light-sensitive RFP, 3D rendering, 150 µm z-stack, 30 sec/stack. See video at. Watch the video on the STELLARIS DLS product page.

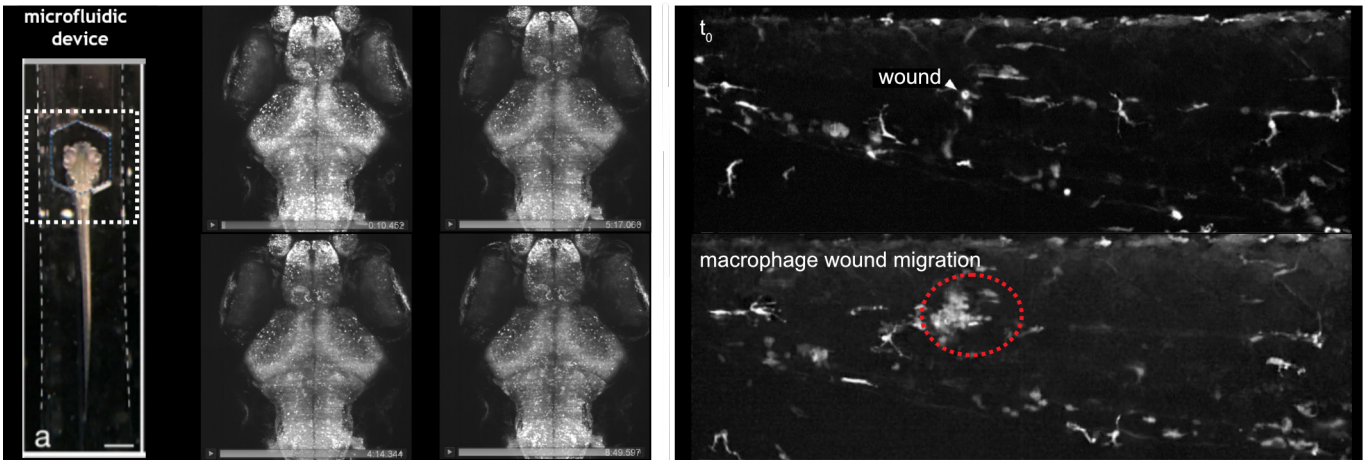

Fig. 13 | **Left:** 6 dpf Tg(elavl3:H2B-GCaMP6s) zebrafish larva held in a microfluidic device depicting nuclear-localized GCaMP6s throughout the larva's brain. Adapted from Mattern et al. Communications Biology (2020) DOI: 10.1038/s42003-020-1029-7. **Right:** Macrophages in the tail of a 4-day old zebrafish embryo after wounding (mpeg1:Kaede). Cells involved in the immune response are attracted to this manipulation site, red circle. Sample courtesy of Francesca Peri, EMBL Heidelberg, Germany.

Fig. 14 shows a *Silene sendtneri* sample on a glass-bottom, 35-mm dish. The roots are placed between a U-shaped glass capillary to direct their geometry between the TwinFlect mirrors. This straightforward sample preparation together with the DLS module allowed 26 hours of imaging of the endogenous root signals (Chlorophyll) and plant cell walls through reflection signals.

Thus, the STELLARIS DLS offers the flexibility of all live imaging-confocal capabilities from STELLARIS, plus the additional flexibility to benefit from light sheet microscopy on an inverted geometry.

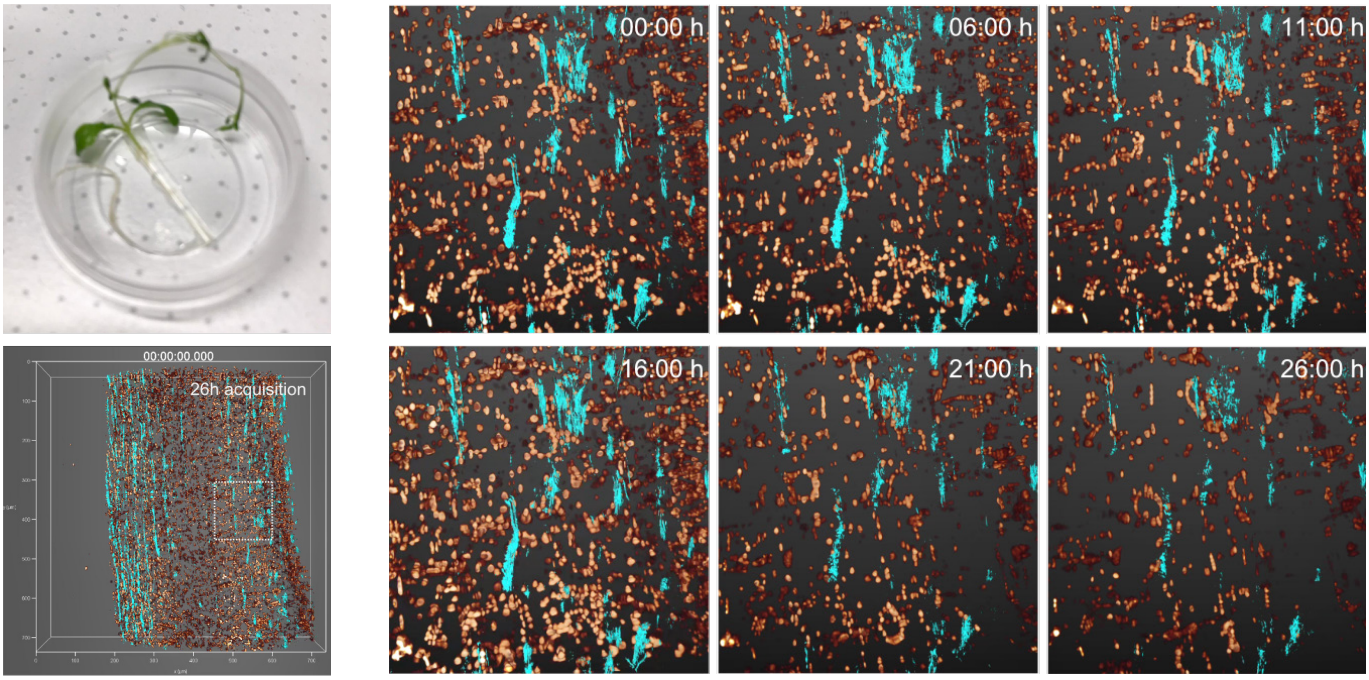

Fig. 14. | *Silene sendtneri*. **Top left:** plant preparation on a 35mm dish. **Bottom Left:** complete view of the root section. **Right panels:** zoomed in time points depicting endogenous fluorescence of chloroplasts and cell wall reflection microscopy. Total imaging time 26h00. Sample courtesy of Erna Karalija, University of Sarajevo.

Nanoscopy meets cellular dynamics

Even if confocal microscopy can already provide excellent resolution, there is an intrinsic optical limit to the achievable resolution when focusing a beam due to the diffraction of light. This limit is roughly 250 nm laterally and 350 nm axially for high numerical aperture (NA) objective lenses. Due to this effect, the image of a single point of light is spread out from its center into a pattern known as an Airy disk. Using mathematical deconvolution, it is possible to further improve the resolution up to a factor of two.

The development of STED super-resolution enabled the diffraction barrier to be circumvented by optical means and represented a breakthrough in the ability to observe subcellular details down to a few tens of nm laterally and below 100 nm axially.

The STED principle relies on the ability to control the emitting and dark states of a fluorophore. The emission of fluorophores within a diffraction-limited spot is confined to a sub-diffraction region by overlaying a donut-shaped laser beam of appropriate wavelength (STED beam) onto the excitation beam. The fluorophores under the influence of the STED beam return to the ground state by stimulated emission before spontaneously emitting a photon and the effective focal volume is reduced below the diffraction limit. The extent of the resolution improvement is linked to the applied STED laser power and this has made it challenging to apply this technology in live cell imaging.

Pioneering work exploiting fluorescence lifetime to enhance STED performance and overcome issues associated with intensity-based approaches (Lanzanò, Coto Hernández et al. 2015), mainly related to the high light dose needed to achieve complete depletion and artifacts derived from adaptive illumination. Yet these improvements did not improve the slow acquisitions needed in traditional STED approaches. Leveraging on our fast FLIM and lifetime-based technologies (Alvarez, Widzgowski et al. 2019, Roberti, Lopez et al. 2020), Leica Microsystems introduced TauSTED, a new approach to achieve high quality, multicolor STED in 2D and 3D, compatible with live cell imaging of highly dynamic processes. It combines optical signals from STED with physical information from the fluorescence lifetime acquired at typical confocal speeds. The Leica approach uses phasor analysis in a novel way and works in an automated manner, enabling increased STED resolution

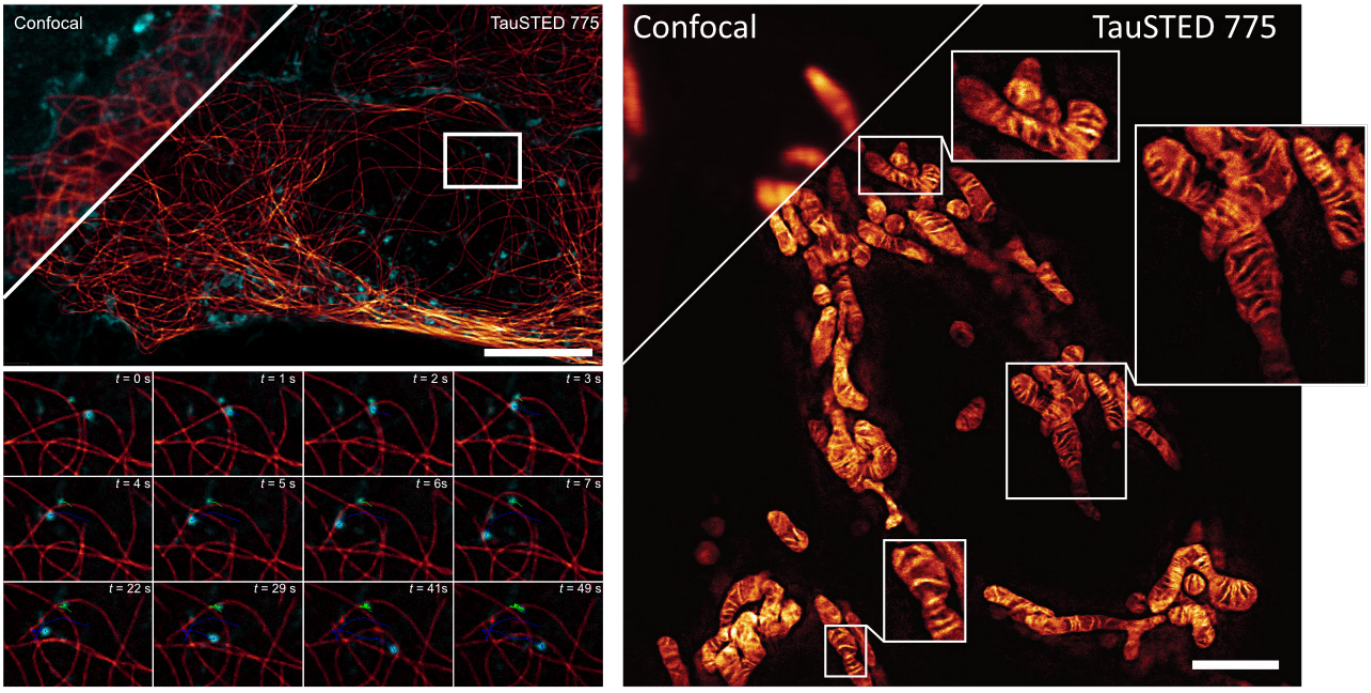

Fig. 15 | Live cell TauSTED with STED at 775 nm. **Top left:** Two-color live cell TauSTED of cytoskeleton (labeled with SPY-620, glowscale) and vesicles (labeled with a 594-nm-excitable fluorophore coupled to wheat germ agglutinin, cyan). STED was performed at low light dose with a single STED line (775 nm). Scale bar: 5 µm. The cell was imaged over time at 1 frame per second to characterize the fast dynamics. **Bottom left:** The montage shows a selection of time points from the inset; three individual vesicles were tracked at high speed (red, green, and blue traces). TrackMate plugin for Fiji was used (Tinevez et al. 2017). A movie is available at https://www.leica-microsystems.com/tausted-cell-dynamics. **Right:** HeLa cells stably expressing COX8A-SNAP labeled with SiR-BG. Sample courtesy of T. Dellmann and A. Garcia, CECAD, Köln, Germany. Cell line originally from S. Jakobs (Stephan et al. 2019) . Scale bar: 2 µm.

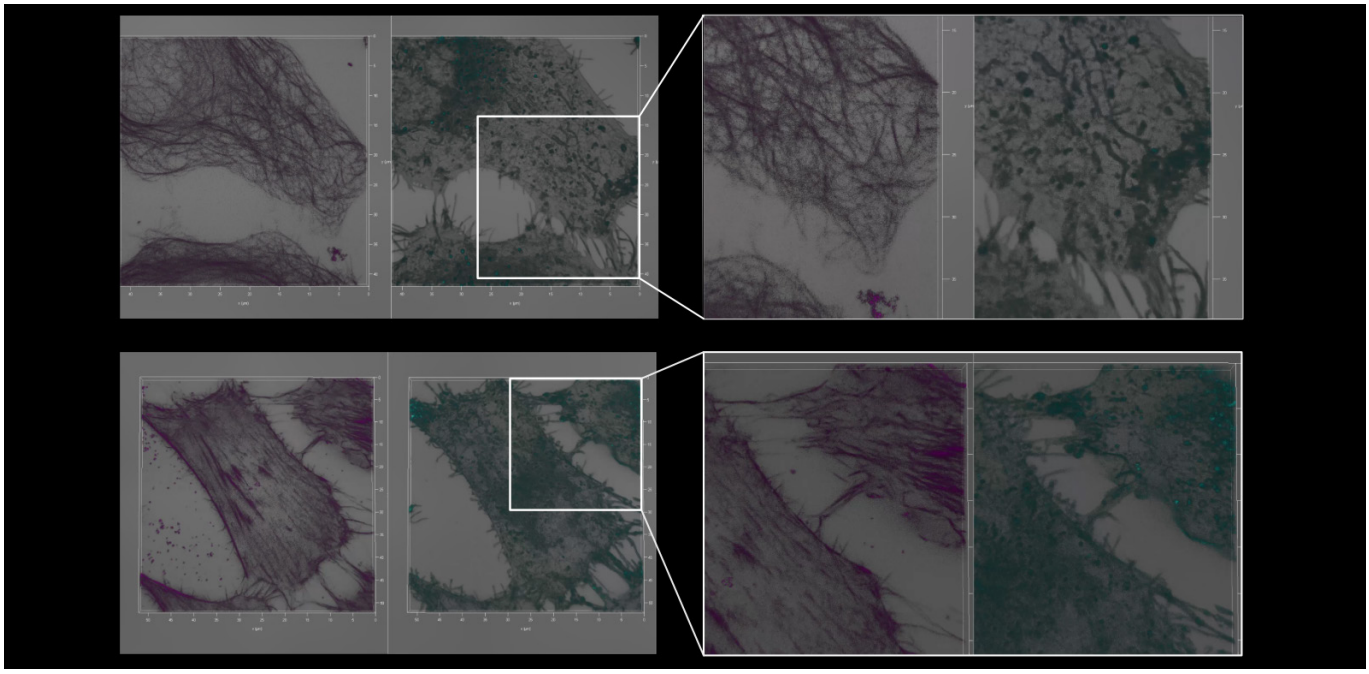

Fig. 16 | Fast-volumetric 2-color TauSTED. **Top:** SiR-tubulin (magenta) and internal cellular membranes (Nile red – cyan). **Bottom:** SiR-actin (magenta) and internal membranes (Nile-red -cyan).

and elimination of uncorrelated background noise, even at low excitation and STED light doses. The details of this approach and examples can be found in the published literature (Alvarez, Schwarz et al. 2021, Cerutti, D'Amico et al. 2021).

TauSTED allows access to STED information as soon as the STED beam has an effect on the lifetime of the fluorophores in the sample. The first benefit from this approach is that there is no photon loss compared to gated STED. It is, therefore, not needed to increase the excitation power to compensate for the loss of signal-to-noise. The other key development with this approach is the possibility to perform STED experiments with STED laser depletion powers as low as 2%. This added modularity of STED powers creates the needed flexibility to tackle live imaging experiments. With TauSTED, the STED acquisition can be performed at the same excitation power as the regular confocal images. STED information can be accessed with minimal STED depletion powers.

This combination is key to achieve proper temporal sampling to track fast biological processes, such as vesicle and actin dynamics seen in Fig. 15 (video available at https://www.leica-microsystems.com/tausted-cell-dynamics). Approaching STED with low light doses benefits applications where light sensitivity is a known limiting factor, such as mitochondria due to their function and the electron transport chain. Imaging them at high resolution, hence, represents a great challenge and their integrity is a good gauge of cellular integrity and phototoxicity. Fig. 15 shows the mitochondria cristae well defined on live cell TauSTED (Stephan, Roesch et al. 2019, Alvarez, Schwarz et al. 2021).

As already discussed for other general topics, there are times when volumetric speeds are needed to follow biological processes. Speed and resolution are fundamental opposites: one can generally image objects in great detail or fast. These limits come in part from the number of photons needed to generate an image and how many of them can be harnessed per frame rate. As stated in the previous sections, for live imaging it is desirable to have the lowest possible excitation power. Researchers would avoid high genetically tagged overexpressing constructs to maintain the integrity of biological processes and have to be careful with the concentrations of organic dyes to avoid phototoxicity. All these precautions, plus the added need to follow the temporal dynamics of such specimens, means the imaging conditions are the opposite of the parameters used to acquire super-resolution images. Therefore most super-resolution techniques struggle when used for live imaging (Tosheva K. et al. 2020). As TauSTED can function at the same speeds as confocal microscopy, it is possible to speed up the TauSTED acquisitions when needed. Fig. 16 shows a three-dimensional two-color TauSTED example acquired at a volume every 9.4 seconds. Here the resonant scanner allows the user to have the proper speed, keeping up with the large FOV and the high pixel density needed for nanoscopy.

Lifetime-based imaging – functional imaging in live cells

Advance imaging approaches to extract functional information from microscopy experiments rely on the quantification of intensity signals. When fluorescence is emitted, one of the physical dimensions is the intensity (given by the number of photons emitted), but it is also possible, with the appropriate system, to also measure the fluorescence lifetime. This additional dimension is characteristic for a given fluorophore and its chemical micro-environment (Fig. 19, Valeur 2001).

Fluorescence lifetime imaging microscopy (FLIM) up until recently has been reserved to specialized laboratories with complicated setups that required slow acquisition times not easily compatible with the dynamics of processes observed in live imaging experiments. Leica Microsystems introduced a novel concept for FLIM acquisitions, Fast Lifetime CONtrast (FALCON), that overcame these limits enabling video-rate FLIM acquisition (for more detail, see Alvarez, Widzgowski et al. 2019). This approach is built on pulsed excitation given by the WLL, the intrinsic photon counting characteristics of the Power HyD detectors, and the scan head electronics (FPGA) that enable the high-count rates used to obtain photon-arrival-time information.

Building on the strengths of the FALCON technologies, STELLARIS introduced a new set of lifetime-based tools to leverage the lifetime dimension of fluorescence signals to enhance the core confocal capabilities of this new generation confocal system (for details see Roberti, Lopez et al. 2020). All WLL STELLARIS systems have access to the TauSense tools without the need for additional hardware or complicated acquisition strategies.

These lifetime-based implementations allow users to benefit from the lifetime dimension at confocal speeds, making it possible to acquire this extra-information layer in parallel without negatively impacting the speed or excitation-light power needing during imaging. They are an ideal addition for live imaging experiments.

TauSense tools for live imaging

TauContrast

TauContrast makes it possible to add an Average-Arrival-Time (AAT) image together with an intensity image (Fig. 17). In this example of the root-hypocotyl-junction of Arabidopsis thaliana, there is contribution to the fluorescence intensity from life-Act Venus, the chloroplasts (endogenous fluorescence), and propidium iodide. The intensity-only image (top) shows all of the photons that reached the detector and the corresponding three-dimensional image. The corresponding TauContrast image is able to show, due to the AAT values, the spatial distributions and contributions for each of the three signals. TauContrast can be an easy way to monitor lifetime-based changes to intensity signals during a pulse-chase experiment or compared to a control within an experimental group.

TauGating

As its names indicates, TauGating makes it possible to generate time-gated channels. These are detection windows containing the photon information on a given digital time gate. These windows are generated on the fly from the photon-arrival-time (AT) information. As these gates rely on a digital sorting of the detected signals, no photons are lost. It is possible during acquisition to discard signals outside a given gate or to visualize them on an additional channel.

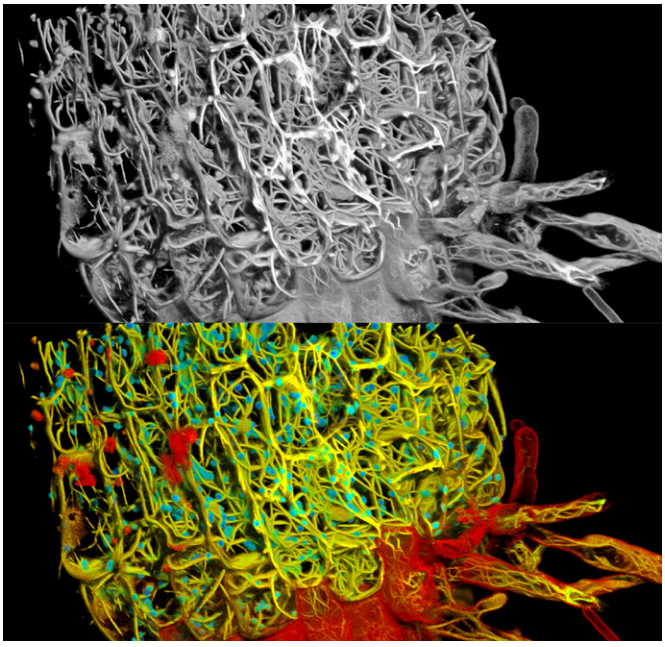

Fig. 17 | TauContrast - Intensity **(top)** and lifetime-based **(bottom)** image of *Arabidopsis thaliana* root expressing an actin fluorescent marker and labeled with propidium iodide. Actin, membranes, and chloroplasts show different characteristics as observed in the lifetime-based image (Sample courtesy of M. Krebs, COS, University of Heidelberg, Germany).

In the fast-volumetric imaging section, the endogenous nematosomes were separated from the dextran signals with this approach (Fig. 6). There is a number of signals with specific lifetime signatures that can be separated from other fluorescence of interest. For example, this is the case for chlorophyll, native pigments in developing zebrafish, pigments in *C. elegans*, as well as SHG and THG in multiphoton imaging. This is a valuable tool for live imaging, because it enables the imaging of fluorescence of interest against signals not easily avoided because of their spectral properties.

TauSeparation

One could be tempted to use the temporal gates afforded by TauGating to separate fluorophores with different lifetime profiles. Nevertheless, the nature of the fluorescence emission makes this ineffective. Indeed, a given fluorescence species will generate photons distributed across a large portion of the lifetime scale. Fluorescence lifetimes have to be seen not as being generated at a single particular time gate, but rather as gaussian signals with a particular lifetime behavior.

TauSeparation allows for the generation of a distribution of lifetime components. From this distribution, one can generate separation channels for the photon arrival times which are used to separate distinct fluorophore signals.

One key difficulty faced by researchers using animal models is that a fluorescence marker (most often GFP) is used to track the specific mutations of interest or genetic markers. This approach is very practical to ensure that the proper genetic background is being used during the experiments. Nevertheless, the use of such genetic tagging blocks that spectral window from any further use. This becomes problematic when it is needed to use fluorescence sensors with emissions overlapping the fluorophore tracking the mutant backgrounds. For example, this is the case for p53 FITC based sensors and GFP or JC-1 which are used to assess mitochondria potential.

In Fig. 18 a cell stably expressing LifeAct-mNeonGreen was also labeled with MitoTracker green, NucRed, and SiR-Tubulin. The intensity-only images from this combination of fluorophores will yield only 2 intensity channels (Fig. 18 top). By using TauSeparation, all four signals are well defined (Fig. 18 bottom).

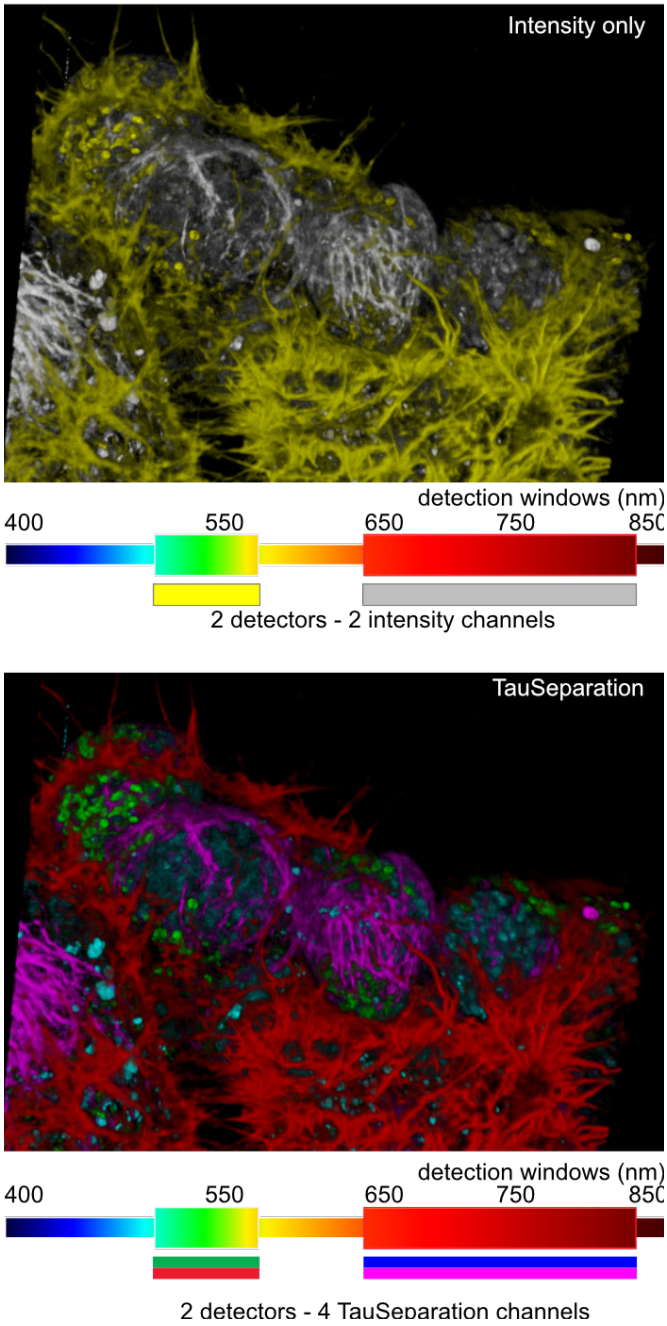

Fig. 18 | TauSeparation: NE-115 cells expressing LifeAct-mNeonGreen (top-yellow, bottom - red) and labeled with MitoTracker green (top – yellow, bottom – green), NucRed (top – grey, bottom – cyan), and SiR-Tubulin (top – grey, bottom – magenta).

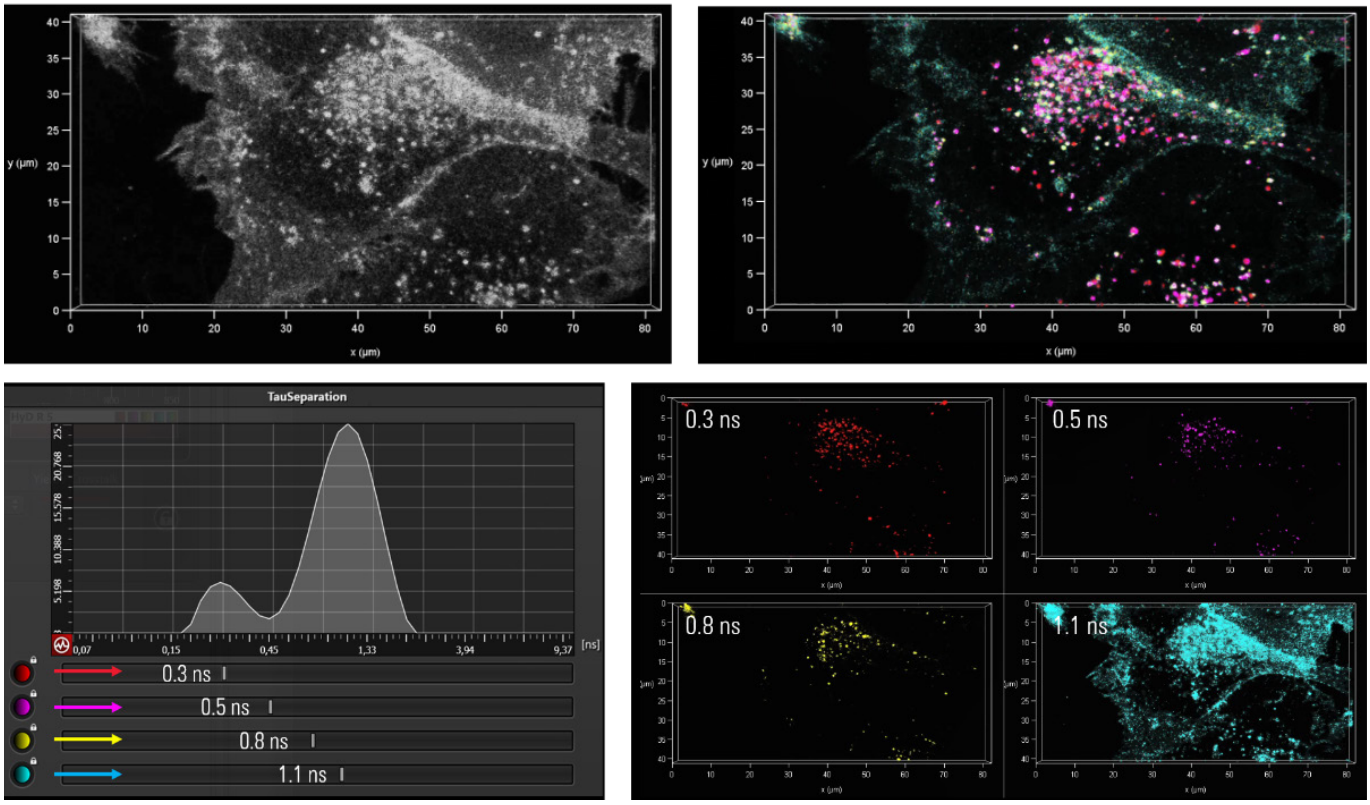

Fig. 19 | NIR 750 signal showing all cellular membranes. **Top left:** Intensity-only image. **Bottom left:** distribution of lifetime components with selected separated channels. **Top right:** Merged separated channels. **Bottom right:** Separated channels showing distinct lifetime signatures.

Another case where the potential of TauSeparation for live imaging becomes apparent is when looking at cellular membranes. When most membrane dyes come into contact with cells, a portion of them start being internalized through the endosomic pathway. The vesicles in this pathway have the particularity of distinct pH levels with diminishing pHs as the vesicles "mature" from the cytoplasmic membranes - from early and mid-endosomes to late endosomes and finally lysosomes.

In each of these pH steps a fluorophore would exhibit different lifetime behavior due to the changing microenvironment. This can be easily observed by looking at the corresponding TauContrast image. As the different maturation states correspond to distinct biological networks, it would be suitable to be able to classify the different signals by which part of the endocytic pathway they correspond to.

TauSeparation enables the distribution of signals into distinct channels (Fig. 19 bottom right).

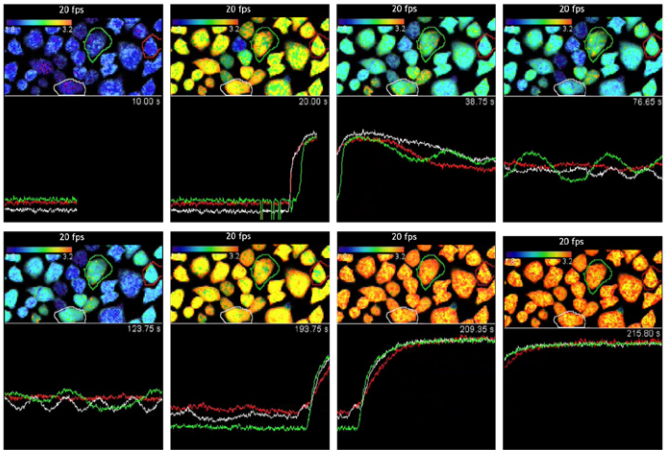

Fig. 20 | OG488-BAPTA1 AM, mammalian cells stimulated by histamine. In the 20-fps measurement, ionomycin was added to boost the calcium levels to the maximum at the end of the experiment. Courtesy of Kees Jalink, Bram van den Broek, NKI, Amsterdam, the Netherlands.

Access to classical FLIM tools for live imaging with FALCON

In addition to the TauSense tools, STELLARIS 8 also gives the possibility to retain the photon-arrival-time information after acquisition and use classical FLIM tools to analyze the acquired images.

The FLIM data here can be used in conjunction with biosensors to quantify molecular changes at the cellular and subcellular levels. Fig. 20 show one such example following fast calcium oscillations at 20 fps. The quantitative nature of lifetime changes allows the intrinsic challenges of following such changes from the intensity-only signals to be avoided.

Another key set of measurements that are particularly well suited for FLIM are Förster-resonance-energy-transfer (FRET, Förster 1960) experiments to probe protein-protein interactions or use FRET biosensors.

Here, FALCON provides access to advanced tools to use the fluorescence lifetime decays and fitting tools to access FRET efficiency and binding measurements (fraction of interaction donor), as well as non-fitting analysis of lifetime distributions using the phasor approach.

As FALCON was developed with fast acquisitions in mind, it is compatible with the live imaging needs for high temporal dynamics, multi-color capabilities, and dim signals. With STELLARIS the phasor has implemented a new filtering option, the wavelet filter to ensure better handling of photon sparse images, such as the ones produced with live cells and other delicate live specimens (Wang, Hecht et al. 2021).

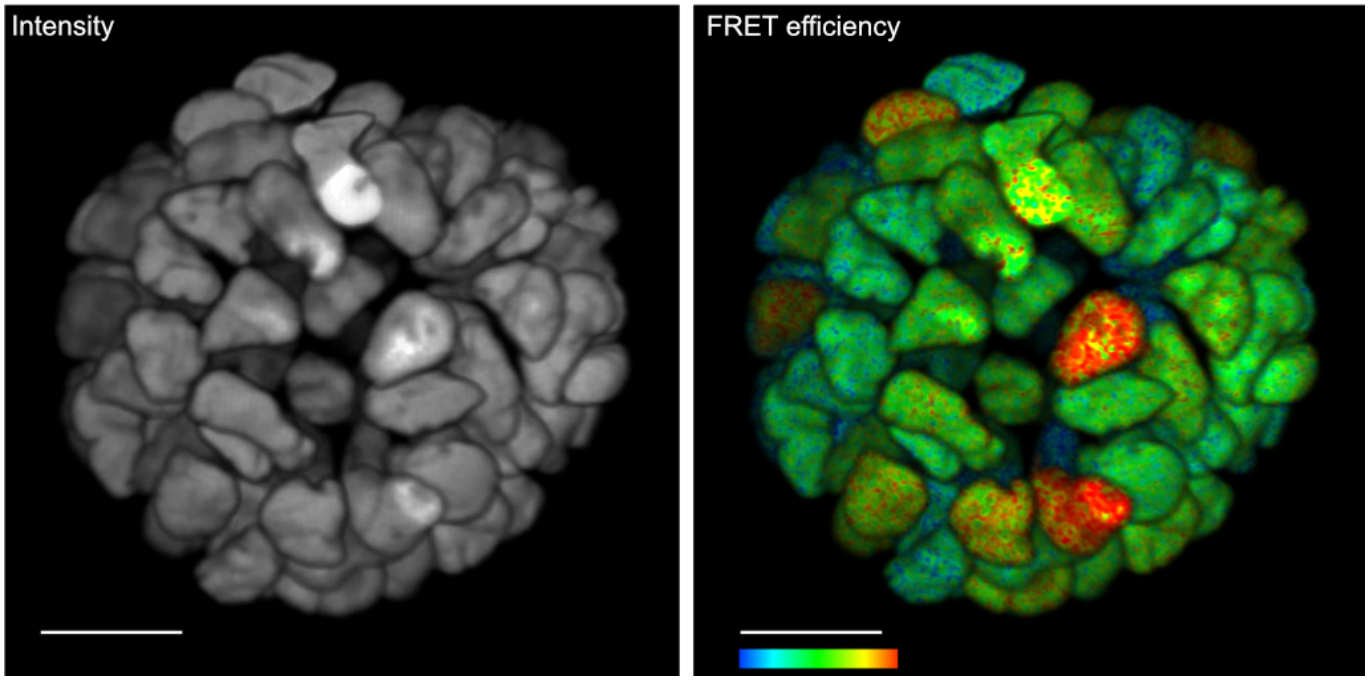

Fig. 21 | FLIM on a live 3D patient-derived cancer organoid. Monitoring cancer-derived increase of signal transduction activity in live organoids with an ERK FRET-FLIM biosensor. **Left:** Corresponding fluorescence intensity image with no functional information. **Right:** Functional information showing FRET efficiency of the ERK biosensor. Higher FRET efficiency means higher ERK activity. Color bar range: 2-12% FRET efficiency. Scale bar: 20 µm.

Phasor separation in FALCON – a new frontier for signal unmixing

One additional FALCON tool introduced with STELLARIS is phasor separation. With the phasor approach, lifetimes are depicted in a two-dimensional polar plot. Here the lifetime fingerprints from the image appear like clouds, giving a visual distribution of the various lifetime components present in the image. By selecting the different populations, FALCON is able through the phasor algebra (Digman, Caiolfa et al. 2008) to separate the chosen signals into phasor-separated channels.

This lifetime separation approach can be used on fixed specimens when there is no available spectral option. It is nevertheless with live imaging that this new approach can advance imaging to a new level. It is possible for example to have multiple genetically tagged proteins that can be excited with a single laser line and detected with a single spectral window, but separated through lifetimes.

Fig. 22 shows four neuronal types in *C. elegans*, each expressing a red shifted fluorescence protein. Here a single excitation and a single emission window is sufficient to explore such rich sample. In any traditional spectral-only microscopy approach, one would need to excite and image 4 fluorophores separately, multiplying by four the excitation energy, but also the time needed to image the sample. With the proper experimental design, lifetime-based approaches, such as this, can open the door to monitoring many more cellular processes, proteins, or structures simultaneously.

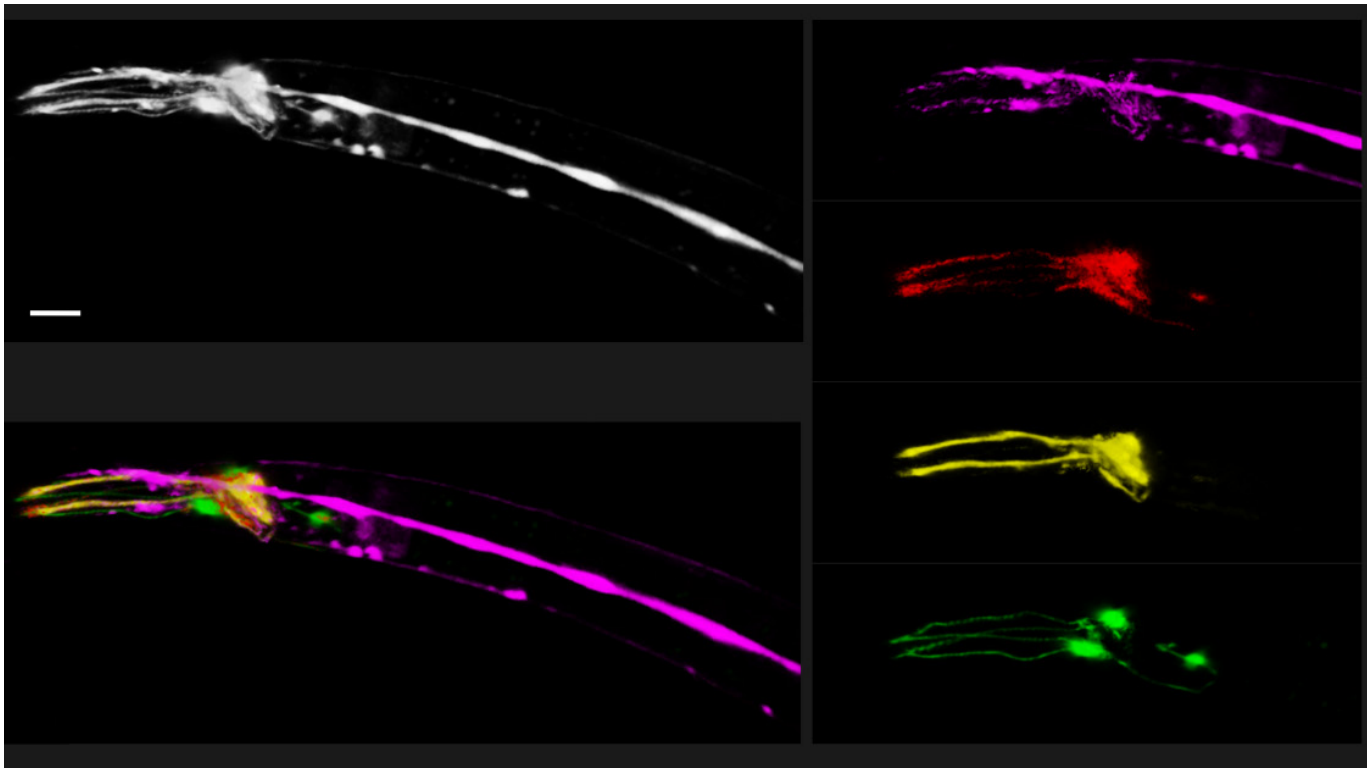

Fig. 22 | 3D confocal image of C. elegans neurons labeled with four red fluorescent proteins. **Top left:** Intensity only. **Bottom left:** Merged phasor-separated signals **Right:** Phasor-separated channels. Scale bar: 20 µm..

From the incubator to the microscope: Key aspects of cell viability & physiological environments

Physiological Conditions Under the Microscope

An important basis for experimental science is the ability to replicate a set of observations under the same conditions as many times as required to prove a hypothesis. Accordingly, while performing biological experiments, environmental control is mandatory, not only to reduce the variability between experiments, but also to guarantee the viability of the specimens. In life sciences, the capacity to replicate a mechanism under physiological conditions is key to the relevance of the observed results.

Temperature

Viability of live organisms at each scale (organism, cells, molecules) is directly dependent on temperature. The homeostasis is finely linked to how well the temperature can be controlled. Indeed, many organisms have a basal behavior that reacts promptly with variations in temperature. Depending on the application, a small or a large volume around the organism can be kept at a defined temperature. For small volumes, stage-on-top incubators are the first choice. For large volumes, microscope-cage incubators should be considered.

In addition to the biological cultured condition, the temperature also has a significant effect on the mechanical stability of a microscope. It is then also important when doing long time-lapse investigations to ensure that the temperature around the sample remains constant. Temperature stability helps avoid sample drift and allow the observation of cellular processes over long-time scales.

Carbon Dioxide (CO_2) Levels and pH of the Medium

A pH of 7.2–7.4 provides optimal growth conditions for most mammalian cells. Stability of the pH of the culture medium is often maintained by buffering systems. The pH of the medium is dependent on the delicate balance of dissolved carbon dioxide (CO_2) and the buffering system. Changes in the atmospheric CO_2 can alter the pH of the medium. To avoid any pH changes, it is necessary to supplement the incubator with exogenous CO_2 or use so-called CO_2 independent media. When using media buffered with CO_2-dependent buffers, 4 – 10% CO_2 in air is often used for most cell culture experiments. Each medium has a recommended CO_2 tension and buffer concentration to achieve the correct pH and osmolality. One should refer to the media manufacturer's instructions for more information. For all needed CO_2 concentrations, the given incubators can be combined with the appropriate gasification modules. In general, only the stage-top chamber is filled with CO_2.

Fig. 23| STELLARIS 5 DLS system with a transparent cage incubator to keep the temperature constant during long acquisitions.

Humidity and Evaporation

Evaporation from cell culture media during live cell imaging experiments should be avoided as constant levels of salts, nutrients, and other cell culture medium components are essential for reproducible cell behavior. This parameter is also crucial for consistent and reliable in vitro results. Any level of evaporation from the cell culture media increases the substance concentration in the medium. Any such changes can dramatically influence the vital functions of living cells. Some consequences of changing humidity or evaporation can be an increased or decreased proliferation, up- and down-regulation of gene expression, and induction of apoptosis/cell death. This can happen particularly fast in low-volume cultures. A constant and high level of humidity (>90% RH) in the stage-top incubator can be one of the keys to artifact-free results from live imaging. To assure the right humidity conditions, the given incubators can be combined with active or passive humidification modules.

Oxygen (O2) Levels

For live imaging assays, the oxygen (O2) concentration is another important parameter that needs to be controlled. The O2 levels in healthy body tissues and our blood range from 14% in the alveoli to 5% in peripheral tissues. Some biological processes cannot be observed unless the appropriate oxygenation level is used (Alvarez, Kovačič et al. 2016). In pathological situations, the oxygen levels can be even lower, especially in tumor tissue. Cancerous tissue is characterized by markedly low O2 levels that range from approximately 4% to a minimum below 0.5%. In contrast, the O2 concentration at normal atmospheric pressure is around 20–21%. Depleting the atmospheric O2 concentration is relevant for bringing the amount of oxygen to physical levels or studying the effects of hypoxia. In addition, an oxygen-depleted environment can also reduce phototoxicity effects during imaging. For all needed O2 conditions, whether hypoxia or hyperoxia is required, the given incubators can be combined with the appropriate gasification modules.

Condensation

Humidity in ambient air can lead to condensation on all surfaces, especially on the lids of cell culture vessels. If these surfaces are in the opti¬cal pathway, small water droplets will cause light scattering. This di¬minishes the optical quality of transmitted light microscopy (i.e., phase contrast and DIC). To ensure the highest image quality, condensation on any surface must be prevented during live cell imaging experiments.

Concluding remarks

Planning and executing live imaging experiments require careful consideration of multiple factors in order to get meaningful results. These considerations start with the experimental design, sample preparation, environmental conditions, and finally imaging parameters (Wait, Reiche et al. 2020). The instrumentation developments that have led to the STELLARIS live imaging capabilities presented in this guide, together with new, less invasive, more physiological labeling approaches, promise exciting discoveries.

References

Alvarez, L. A., et al. (2016). "NADPH oxidase-derived H2O2 subverts pathogen signaling by oxidative phosphotyrosine conversion to PB-DOPA." Proceedings of the National Academy of Sciences of the United States of America **113**(37).

Alvarez, L. A. J., et al. (2021). "TauSTED: pushing STED beyond its limits with lifetime." Nature Methods **18**(6).

Alvarez, L. A. J., et al. (2019). "SP8 FALCON: a novel concept in fluorescence lifetime imaging enabling video-rate confocal FLIM." Nature Methods **20**: 2-4.

Alvarez, L. A. J., et al. (2019). SP8 FALCON: a novel concept in fluorescence lifetime imaging enabling video-rate confocal FLIM. Nature Methods. **20**: 2-4.

Bindels, D. S., et al. (2017). "mScarlet: a bright monomeric red fluorescent protein for cellular imaging." Nature Methods **14**(1): 53-56.

Cerutti, E., et al. (2021). "Evaluation of sted super-resolution image quality by image correlation spectroscopy (QuICS)." Scientific Reports **11**(1): 20782.

Davaji, B., et al. (2019). "Microscale direct measurement of localized photothermal heating in tissue-mimetic hydrogels." Scientific Reports **9**(1): 6546.

Digman, M. A., et al. (2008). "The Phasor Approach to Fluorescence Lifetime Imaging Analysis." Biophysical Journal **94**(2): L14-L16.

Elliott, A. D. (2020). "Confocal Microscopy: Principles and Modern Practices." Current Protocols in Cytometry **92**(1): e68-e68.

Förster, T. (1960). "Transfer Mechanisms of Electronic Excitation Energy." Radiation Research Supplement **2**.

Galvao, J., et al. (2014). "Unexpected low-dose toxicity of the universal solvent DMSO." The FASEB Journal **28**(3): 1317-1330.

Gautier, A., Juillerat et al. (2008). "An Engineered Protein Tag for Multiprotein Labeling in Living Cells." Chemistry and Biology **15**(2): 128-136.

Greenwald, E. C., et al. (2018). "Genetically Encoded Fluorescent Biosensors Illuminate the Spatiotemporal Regulation of Signaling Networks." Chemical Reviews **1**18(24): 11707-11794.

Kilgore, J. A., Dolman et al. (2013). "A Review of Reagents for Fluorescence Microscopy of Cellular Compartments and Structures, Part II: Reagents for Non-Vesicular Organelles." Current Protocols in Cytometry **66**(1): 12.31.11-12.31.24.

Kilgore, J. A., Dolman et al. (2014). "A review of reagents for fluorescence microscopy of cellular compartments and structures, Part III: Reagents for actin, tubulin, cellular membranes, and whole cell and cytoplasm." Current Protocols in Cytometry(SUPPL.67).

Köster, I. and P. Haas (2015). "Light Sheet Microscopy Turned Vertically." Optik & Photonik **10**(4): 39-43.

Lanzanò, L., et al. (2015). "Encoding and decoding spatio-temporal information for super-resolution microscopy." Nature Communications **6**(1): 6701.

Lecoq, J., et al. (2019). "Wide. Fast. Deep: Recent Advances in Multiphoton Microscopy of In Vivo Neuronal Activity." J Neurosci **39**(46): 9042-9052.

Lemon, W. C. and K. McDole (2020). "Live-cell imaging in the era of too many microscopes." Curr Opin Cell Biol **66**: 34-42.

Los, G. V., et al. (2008). "HaloTag: A novel protein labeling technology for cell imaging and protein analysis." ACS Chemical Biology **3**(6): 373-382.

Lukinavičius, G., Reymond et al. (2014). "Fluorogenic probes for live-cell imaging of the cytoskeleton." Nature Methods **11**(7): 731-733.

Magidson, V. and A. Khodjakov (2013). Circumventing photodamage in live-cell microscopy. Methods in Cell Biology, Academic Press Inc. **114**: 545-560.

Matlashov, M. E., et al. (2020). "A set of monomeric near-infrared fluorescent proteins for multicolor imaging across scales." Nature Communications **11**(1): 239.

Mattern, K et al. (2020) NeuroExaminer:an all-glass microfluidic device for whole-brain imaging in zebrafish Comms Bio, **3** (1) 12

Pawley, J. B. (2006). Handbook of biological confocal microscopy: Third edition.

Reynaud, EG et al. (2008). Light heet-based fluorescence microscopy: More dimensions, more photons, and less photodamage HFSP J **2**(5)

Roberti, M. J., et al. (2020). "TauSense: a fluorescence lifetime-based tool set for everyday imaging." Nature Methods **17**.

Roberti, M. J., et al. (2020). "Application Note: TauSense: the potential of STELLARIS." Nature Methods **17**(09).

Rodriguez, E. A., et al. (2017). The Growing and Glowing Toolbox of Fluorescent and Photoactive Proteins. Trends in Biochemical Sciences, Elsevier Ltd. **42**: 111-129.

Salmon, M., et al. (2020). Endogenous Labeling for Light Microscopy during HIV-1 Immune Responses. Trends in Immunology, Elsevier Ltd. **41**: 1056-1059.

Schweikhard, V., et al. (2020). "Application Note: The Power HyD family of detectors for confocal microscopy." Nature Methods **17**(10).

Sheppard, C. J. R. (2020). "Multiphoton microscopy: a personal historical review, with some future predictions." J Biomed Opt **25**(1): 1-11.

Sheppard, C. J. R. and T. Wilson (1981). "The theory of the direct-view confocal microscope." Journal of Microscopy **124**(2): 107-117.

Sinha, R. P. and D.-P. Häder (2002). "UV-induced DNA damage and repair: a review." Photochemical & Photobiological Sciences **1**(4): 225-236.

Stephan, T., et al. (2019). "Live-cell STED nanoscopy of mitochondrial cristae." Scientific Reports **9**(1).

Sun, T. Y., et al. (2017). "Preclinical Advances with Multiphoton Microscopy in Live Imaging of Skin Cancers." J Invest Dermatol **137**(2): 282-287.

Tebo, A. G., et al. (2021). "Orthogonal fluorescent chemogenetic reporters for multicolor imaging." Nature Chemical Biology **17**(1): 30-38.

Tinevez, J. Y. et al. (2017) "TrackMate: an open and extensible platform for single particle tracking." Methods **115**, 80–90.

Tosheva, K. L., et al. (2020). "Between life and death: strategies to reduce phototoxicity in super-resolution microscopy." J Phys D Appl Phys **53**(16): 163001.

Valeur, B. (2001). Molecular Fluorescence - Principles and Applications.

Verheijen, M., et al. (2019). "DMSO induces drastic changes in human cellular processes and epigenetic landscape in vitro." Scientific Reports **9**(1): 1-12.

Wait, E. C., et al. (2020). Hypothesis-driven quantitative fluorescence microscopy - The importance of reverse-thinking in experimental design. Journal of Cell Science, Company of Biologists Ltd. **133**.

Wan, Y., et al. (2019). "Light sheet Microscopy and Its Potential for Understanding Developmental Processes." Annu Rev Cell Dev Biol **35**: 655-681.

Wang, P., et al. (2021). "Complex wavelet filter improves FLIM phasors for photon starved imaging experiments." Biomedical Optics Express **12**(6): 3463-3473.

Wang, Z., et al. (2021). "Live-cell imaging of glucose-induced metabolic coupling of β and α cell metabolism in health and type 2 diabetes." Communications Biology **4**(1): 1-11.

Weber, M. and J. Huisken (2011). "Light sheet microscopy for real-time developmental biology." Curr Opin Genet Dev **21**(5): 566-572.

Willems, J., et al. (2020). "ORANGE: A CRISPR/Cas9-based genome editing toolbox for epitope tagging of endogenous proteins in neurons." PLOS Biology **18**(4): e3000665.

Leica Microsystems CMS GmbH | Am Friedensplatz 3 | 68165 Mannheim, Germany
Tel. +49 621 70280 | F +49 621 70281028

www.leica-microsystems.com/products/confocal-microscopes

CONNECT
WITH US!